Article

SOURCE DATA | TRANSPARENT PROCESS

THE EMBO JOURNAL

A non-canonical role of the p97 complex in RIG-I antiviral signaling

Qian Hao[1,†], Shi Jiao[1,†], Zhubing Shi[1,†], Chuanchuan Li[1], Xia Meng[1], Zhen Zhang[1], Yanyan Wang[1], Xiaomin Song[1], Wenjia Wang[1], Rongguang Zhang[1], Yun Zhao[1], Catherine CL Wong[1,*] & Zhaocai Zhou[1,2,**]

Abstract

RIG-I is a well-studied sensor of viral RNA that plays a key role in innate immunity. p97 regulates a variety of cellular events such as protein quality control, membrane reassembly, DNA repair, and the cell cycle. Here, we report a new role for p97 with Npl4-Ufd1 as its cofactor in reducing antiviral innate immune responses by facilitating proteasomal degradation of RIG-I. The p97 complex is able to directly bind both non-ubiquitinated RIG-I and the E3 ligase RNF125, promoting K48-linked ubiquitination of RIG-I at residue K181. Viral infection significantly strengthens the interaction between RIG-I and the p97 complex by a conformational change of RIG-I that exposes the CARDs and through K63-linked ubiquitination of these CARDs. Disruption of the p97 complex enhances RIG-I antiviral signaling. Consistently, administration of compounds targeting p97 ATPase activity was shown to inhibit viral replication and protect mice from vesicular stomatitis virus (VSV) infection. Overall, our study uncovered a previously unrecognized role for the p97 complex in protein ubiquitination and revealed the p97 complex as a potential drug target in antiviral therapy.

Keywords antiviral signaling; mechanism; p97-Npl4; RIG-I; ubiquitination
Subject Categories Immunology; Post-translational Modifications, Proteolysis & Proteomics
DOI 10.15252/embj.201591888 | Received 24 April 2015 | Revised 6 September 2015 | Accepted 17 September 2015 | Published online 15 October 2015
The EMBO Journal (2015) 34: 2903–2920

Introduction

Viral infections pose increasing threats to public health throughout the world. Innate immunity serves as the first line of defense in the response against the pathogenic invasion of hosts by viruses. Such responses are usually initiated by the detection of viral nucleic acid via pathogen recognition receptors (PRRs), including Toll-like receptors (TLRs) in the endosome and RIG-I-like receptors (RLRs) in the cytoplasm (Kawai & Akira, 2010; Takeuchi & Akira, 2010; Barbalat *et al*, 2011). TLR family members TLR3, 7, 8, and 9 detect endosomal DNA and RNA viruses, while RIG-I, MDA5, and LGP2 of the RLR family are the sensors specific for cytoplasmic RNA viruses (Nakhaei *et al*, 2009; O'Neill & Bowie, 2010; Kato *et al*, 2011). RIG-I and MDA5 are made up of two tandem caspase activation and recruitment domains (CARDs) at the N-terminus, a central RNA helicase domain containing a conserved DExD/H box, and a carboxyl-terminal domain (CTD) (Kolakofsky *et al*, 2012). The CARDs are required for the interaction of RIG-I (or of MDA5) with its adaptor protein MAVS (also known as IPS-I/CARDIF/VISA), which resides in the mitochondrial outer membrane (Kawai *et al*, 2005; Meylan *et al*, 2005; Seth *et al*, 2005; Xu *et al*, 2005). The association of MAVS with RIG-I as mediated by CARDs results in the activation of the downstream signaling cascades and the eventual production of pro-inflammatory cytokines and type I interferons (Kawai & Akira, 2008). Unlike RIG-I and MDA5, LGP2 lacks N-terminal CARDs and thus fails to induce an antiviral immune response by itself (Onoguchi *et al*, 2011). Instead, LGP2 positively regulates RIG-I- and MDA5-mediated antiviral responses (Satoh *et al*, 2010).

Accurate regulation of innate antiviral immunity ensures that the spread of virus in the host is restricted, and at the same time that the development of autoimmune and/or inflammatory diseases caused by excessive interferon production is prevented. The ubiquitin system has been demonstrated to play a crucial role in precisely controlling RLR-mediated signal transduction (Maelfait & Beyaert, 2012; Oshiumi *et al*, 2012). Activation of RIG-I-mediated antiviral signaling starts with the ubiquitination of RIG-I. Infection by an RNA virus results in a conformational rearrangement of RIG-I that exposes its N-terminal CARDs to solvent (Jiang *et al*, 2011; Kowalinski *et al*, 2011; Luo *et al*, 2011); this exposure leads to the recruitment of the E3 ligases TRIM25 (Gack *et al*, 2007) and Riplet (Gao *et al*, 2009; Oshiumi *et al*, 2009), and these two ligases contribute to the conjugation of K63-linked polyubiquitin chains onto RIG-I. Additionally, unanchored K63-linked polyubiquitin chains also bind to the CARDs (Zeng *et al*, 2010). Both covalently linked and non-covalently bound K63-polyubiquitin chains appear to promote RIG-I antiviral activity. MAVS then recruits a series of E3 ligases essential for the activation of the downstream signaling events. Specifically,

1 National Center for Protein Science Shanghai, State Key Laboratory of Cell Biology, Institute of Biochemistry and Cell Biology, Shanghai Institutes for Biological Sciences, Chinese Academy of Sciences, Shanghai, China
2 School of Life Science and Technology, ShanghaiTech University, Shanghai, China
*Corresponding author. Tel: +86 21 20778066; Fax: +86 21 54921291; E-mail: catherine_wong@sibcb.ac.cn
**Corresponding author. Tel: +86 21 54921291; Fax: +86 21 54921291; E-mail: zczhou@sibcb.ac.cn
†These authors contribute equally to this work

auto-ubiquitination of TRAF6 with K63-linked polyubiquitin chains leads to the recruitment of the TAK1 complex and the subsequent activation of the IKK complex (Xu *et al*, 2005; Yoshida *et al*, 2008; Konno *et al*, 2009), which eventually cause nuclear translocation of the transcription factor NF-κB to activate pro-inflammatory genes (Konno *et al*, 2009; Liu & Chen, 2011; Maelfait & Beyaert, 2012). In parallel, K63 auto-ubiquitination of TRAF3 causes the activation of TBK1 and IKKε, which in turn promote the phosphorylation, dimerization, and nuclear translocation of another transcription factor, IRF3, resulting in the expression of type I interferons (Oganesyan *et al*, 2006; Saha *et al*, 2006; Paz *et al*, 2011).

Proteasomal degradation mediated by K48-linked ubiquitination is involved in the attenuation of RLR signal transduction to terminate sustained immune responses. RNF125, which is characterized as a RING-type E3, suppresses antiviral immune response by inducing the degradation of RIG-I, MDA5, and MAVS (Arimoto *et al*, 2007). Other E3s, those that do not directly associate with their substrates, depend on adaptor proteins to be recruited to their specific substrates. Siglec-G, which is upregulated upon RNA virus infection, interacts with E3 ligase c-Cbl and RIG-I via SHP2, facilitating c-Cbl-mediated K48-linked ubiquitination of RIG-I prior to proteasomal degradation (Chen *et al*, 2013). PCBP2 acts as a negative regulator of RLR signaling, sequestering the HECT domain-containing E3 ligase AIP4 to MAVS and catalyzing the conjugation of K48-linked polyubiquitin to MAVS for degradation (You *et al*, 2009). In addition, Ndfip1 has been reported to enhance MAVS degradation mediated by Smurf-1, which is another member of the HECT E3 ligase family (Wang *et al*, 2012).

p97 (also known as VCP/CDC48) is a member of the type II AAA (ATPase associated with various activities) ATPase family and has been found to participate in a wide range of independent cellular processes including ER- and mitochondria-associated degradation (Ye *et al*, 2001; Jarosch *et al*, 2002; Rabinovich *et al*, 2002; Heo *et al*, 2010; Tanaka *et al*, 2010; Xu *et al*, 2011), autophagy (Ju *et al*, 2009; Vesa *et al*, 2009; Krick *et al*, 2010; Tresse *et al*, 2010), membrane reassembly (Latterich *et al*, 1995; Kondo *et al*, 1997; Hetzer *et al*, 2001; Ramadan *et al*, 2007), protein aggregation (Higashiyama *et al*, 2002; Yamanaka *et al*, 2004; Kobayashi *et al*, 2007; Song *et al*, 2007; Nishikori *et al*, 2008), DNA repair (Partridge *et al*, 2003; Indig *et al*, 2004), cell cycle progression (Cao *et al*, 2003; Fu *et al*, 2003; Ramadan *et al*, 2007; Mouysset *et al*, 2008), sex determination (Sasagawa *et al*, 2009), and neutralization of virus (Hauler *et al*, 2012). Many studies have shown that p97 is recruited, with the help of cofactors including Npl4, Ufd1, p47, UBXD7, and FAF1, to ubiquitinated substrates (Kondo *et al*, 1997; Ye *et al*, 2001; Song *et al*, 2005; Alexandru *et al*, 2008; Meyer *et al*, 2012; Yamanaka *et al*, 2012)—and through its segregase activity, p97 extracts its target proteins from their cellular environments mostly for proteasomal degradation. However, Alexandru and colleagues suggested that p97 may be also involved in the ubiquitination of its substrates (Alexandru *et al*, 2008), indicating that the mechanisms by which p97 targets its substrates for degradation are probably more complicated than previously thought. So far, the exact mechanism by which the p97 complex facilitates ubiquitination of its substrates remains unclear, and it is also unknown whether the p97 complex could bind directly to the non-ubiquitinated substrates.

Previously, we studied the mechanism by which RIG-I signaling is activated (Feng *et al*, 2013). In the current work, we identified a previously unknown role of the p97-Npl4 complex in antiviral response, in which the complex was shown to recruit recruits RNF125 to promote K48-polyubiquitination and degradation of RIG-I. Notably, knockdown of p97/Npl4 resulted in concurrent decrease of RNF125-mediated ubiquitination of RIG-I, instead of accumulation of ubiquitinated substrates as was previously expected. In addition to its classic function of binding ubiquitinated substrates, p97-Npl4 was shown also able to recognize non-ubiquitinated substrates and simultaneously recruit E3 ligase in the process of substrate ubiquitination. Upon viral infection, the interaction between RIG-I and p97-Npl4 was substantially enhanced by the following: (i) a conformational change that exposes the CARDs of RIG-I; and (ii) K63-linked ubiquitination of the CARDs. Meanwhile, administering p97 inhibitors to mice protected them from VSV infection, which further suggests that p97-Npl4 should be considered as a promising target for antiviral therapy. Considering the potential for inhibitors of p97 in treating human cancer and the significance of antiviral treatments in cancer patients (Wang *et al*, 2010; Magnaghi *et al*, 2013), our findings may also provide a mechanistic basis for using p97 inhibitors as both anticancer and antiviral agents.

Results

p97 negatively regulates type I interferon signaling in an ATPase-dependent manner

How the viral RNA sensor RIG-I is activated has been extensively studied. The mechanism by which RIG-I antiviral signaling is turned off remains, however, only partially understood. In this work, we set out to investigate such mechanism by performing mass spectrometry (MS) assays using RIG-I as bait. Our MS analysis indicated p97 to be a potential interaction partner of RIG-I (data not shown). Since p97 is important for the degradation of various proteins, we hypothesized that p97 may also play a role in the control of RIG-I protein turnover and thus antiviral signaling.

To determine whether p97 indeed plays a role in type I interferon response and antiviral immunity, we transfected human embryonic kidney (HEK293T) cells with interferon beta (IFNβ)-containing, IFNβ-positive regulation domain PRDIII and PRDI (PRDIII-I)-containing, and interferon-stimulated response element (ISRE)-containing promoters, as well as p97-specific siRNA targeting its CDS sequence, and then infected the cells with Sendai virus (SeV) to trigger type I interferon signaling. Knockdown of p97 led to dramatically increased IFNβ, PRDIII-I, and ISRE promoter activities (Fig 1A; Appendix Fig S1A). Consistent with these results, the mRNA levels of *IFNB*, *RANTES*, and *ISG56* were greatly upregulated in p97-depleted cells upon SeV infection for different periods of time, compared with the scrambled group (Fig 1B). We obtained similar results in 293T cells as well as mouse embryonic fibroblast (MEF) cells when these cell types were transfected with poly(I:C) or treated with poly(dA:dT) or vesicular stomatitis virus with enhanced green fluorescent protein (VSV-GFP) (Fig 1C and D). Together, these results showed that p97-specific knockdown was able to markedly enhance the type I interferon response.

To further demonstrate a functional correlation between p97 and antiviral immunity, we knocked down p97 in MEF cells and then infected the cells with VSV-GFP at a multiplicity of infection of 2.

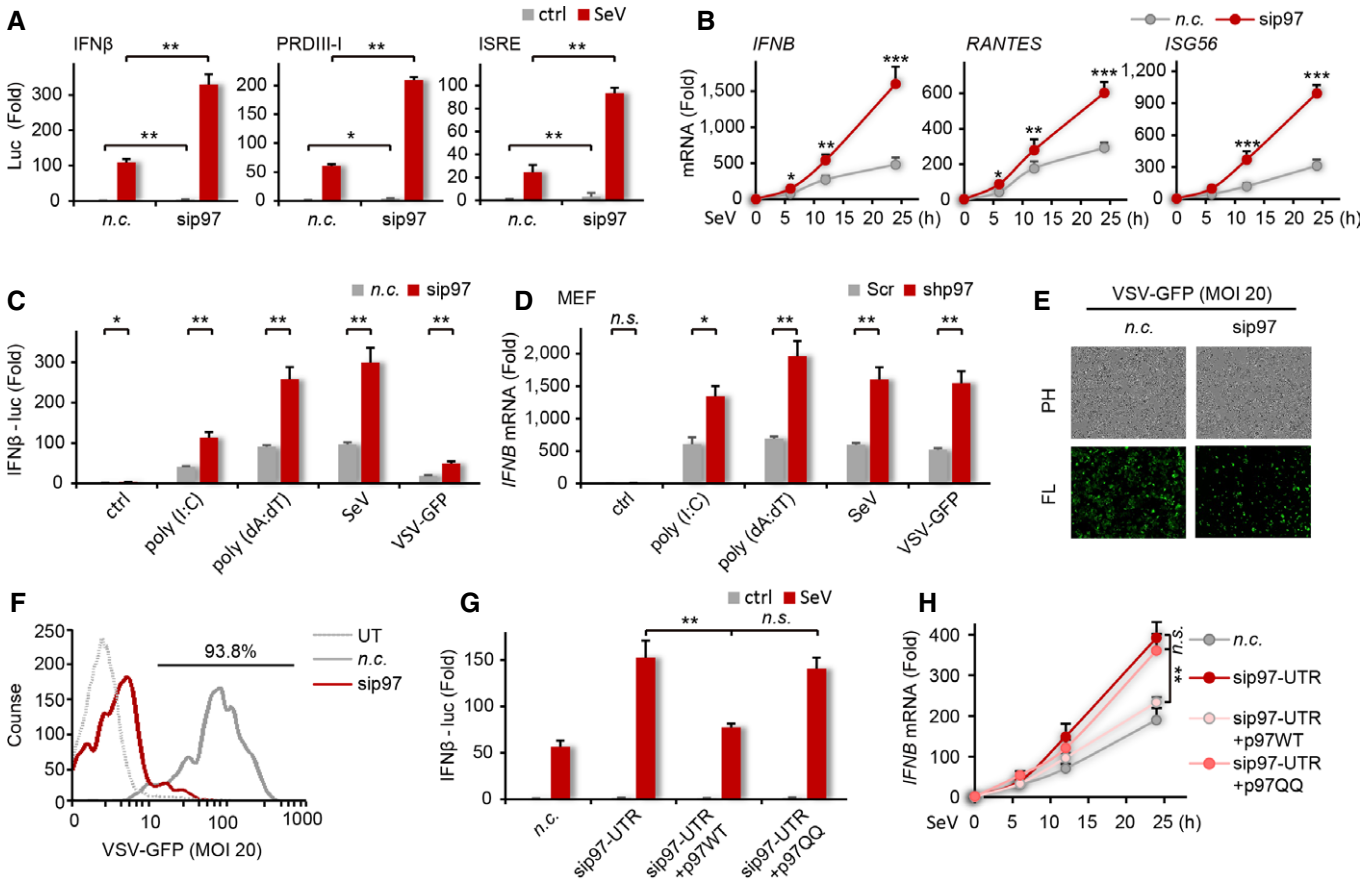

Figure 1. p97 inhibits IFNβ antiviral response in an ATPase-dependent manner.

A Luciferase activities of IFNβ (left), PRDIII-I (middle), and ISRE (right) promoters in HEK293T cells transfected with p97-specific or control siRNA upon SeV infection for 12 h.

B Transcriptional levels of *IFNB* (left), *RANTES* (middle), and *ISG56* (right) in p97-depleted cells after SeV infection.

C, D Luciferase (C) and real-time PCR (D) analyses in p97-depleted cells treated with intracellular poly(I:C), poly(dA:dT), SeV, or VSV-GFP.

E, F Phase-contrast and fluorescence microscopy (E) and flow cytometry (F) assessing the VSV-GFP infection of MEF cells after transfection with p97 siRNA.

G, H Rescue assay for p97 and its mutant on IFNβ transactivation (G) and *IFNB* transcription (H) in p97-depleted cells after SeV infection.

Data information: Error bars represent SD of data obtained in three independent experiments. One-way analysis of variance (ANOVA) and Student's *t*-test were used. n.s., no significant difference; $*P < 0.05$; $**P < 0.01$; $***P < 0.001$ in comparison with control group. n.c., control siRNA; ctrl, saline treated; scr, scramble shRNA; WT, wild-type; p97QQ, a p97 mutant (E305Q_E578Q) defective in ATPase activity; PH, phase-contrast; FL, fluorescence.
See also Appendix Fig S1.

Knockdown of p97 rendered the cells resistant to viral infection, resulting in obviously fewer GFP-positive (virus-infected) cells than those treated with control siRNA (*n.c.*) (Fig 1E). Consistent with these results, flow cytometry showed that relatively few (i.e. only 9%) MEF cells that were transfected with p97-specific siRNA became infected with VSV-GFP, while the vast majority (i.e. 93%) of the MEF cells transfected with control siRNA were observed to be positive for GFP (Fig 1F). Together, these observations indicate that p97 is a negative regulator of antiviral immunity.

Next, we performed a rescue assay to verify the regulatory function of p97 in type I interferon signaling, as well as to address whether such a function depends on its ATPase activity. In cells transfected with p97-specific siRNA targeting its UTR sequence, expression of wild-type (WT) p97 restored the inhibitory effect of p97 on SeV-induced IFNβ luciferase activities and *IFNB* transcription (Fig 1G and H; Appendix Fig S1B). In contrast, the mutant p97QQ (Ye *et al*, 2003), whose ATPase activity is defective, failed to rescue such inhibitory effects. Together, these results confirmed the inhibitory effect of p97 on type I interferon signaling, and demonstrated that such inhibition is dependent on its ATPase activity.

Npl4-Ufd1 is the cofactor of p97 in antiviral immune response

Since multiple cofactors of p97 have been identified to control its differential functions in various cellular processes, we then asked which specific cofactors are required for its negative regulation of antiviral signaling. For this purpose, we measured the luciferase activity of IFNβ and the transcription of *IFNB* in SeV-infected HEK293T cells after knocking down various p97 cofactors including Npl4, Ufd1, p47, and FAF1 (Fig 2A and B; Appendix Fig S2A–D). Depletion of Npl4, but not p47 or FAF1, markedly enhanced IFNβ transactivity and *IFNB* transcription, as did p97 knockdown. In

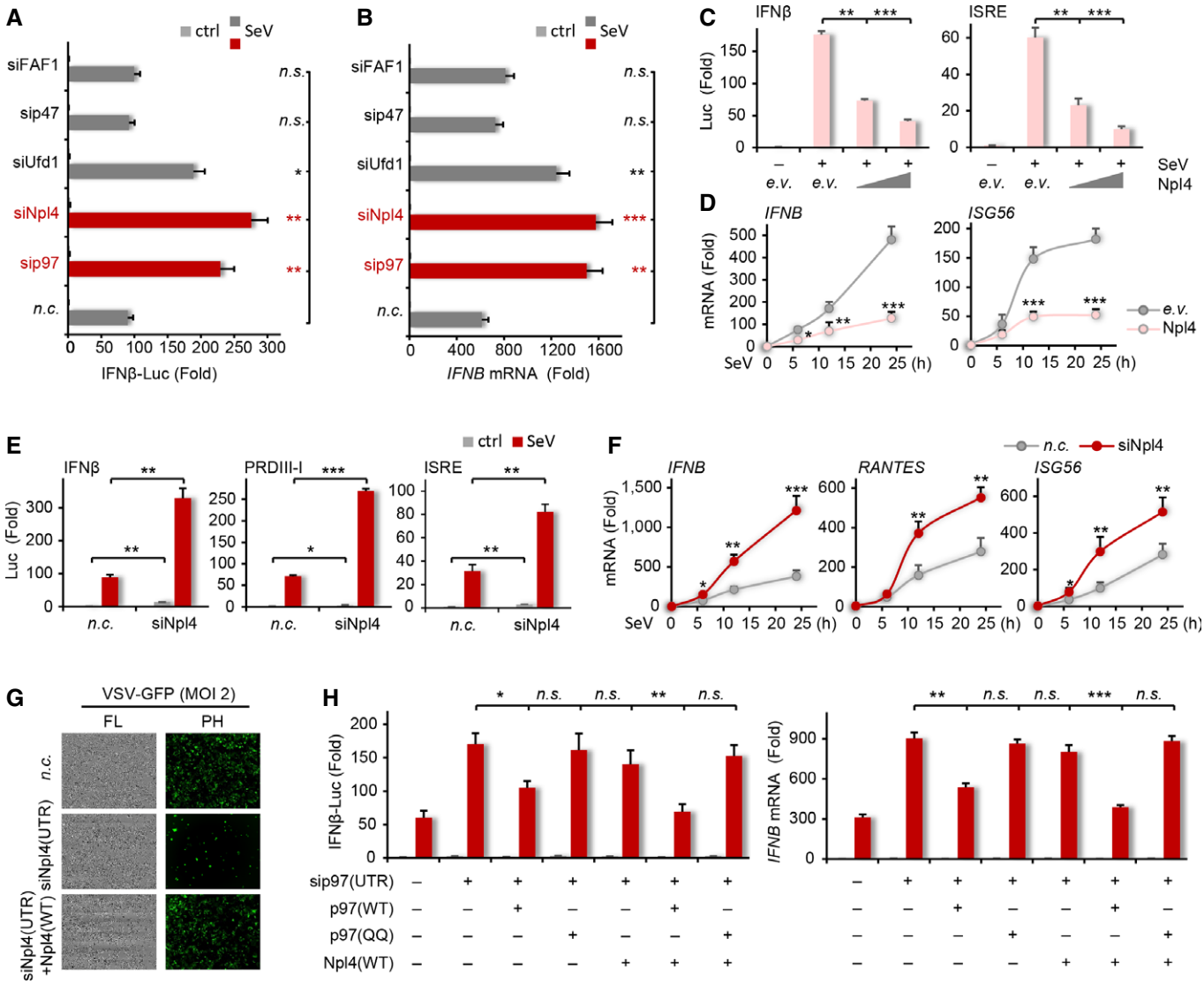

Figure 2. Npl4 cooperates with p97 to suppress IFNβ antiviral response.

A, B Transactivity of IFNβ promoter (A) and transcription of *IFNB* (B) in SeV-infected cells after transfection with indicated siRNA.

C, D Luciferase activities of IFNβ (left) and ISRE (right) promoters (C) and mRNA levels of *IFNB* (left) and *ISG56* (right) (D) in SeV-infected cells transfected with various doses of Npl4.

E, F Luciferase (E) and real-time PCR (F) analyses in Npl4-depleted cells upon SeV treatment.

G Rescue assay in Npl4-knockdown MEFs after infection with VSV-GFP.

H IFNβ transactivation and *IFNB* transcription in sip97 cells transfected with the indicated plasmids.

Data information: Error bars represent SD of data obtained in three independent experiments. One-way analysis of variance (ANOVA) and Student's *t*-test were used. n.s., no significant difference; $*P < 0.05$; $**P < 0.01$; $***P < 0.001$ in comparison with control group. e.v., empty vector. Other abbreviations as in Fig 1. Wedge represents increasing amounts of plasmids.
See also Appendix Fig S2.

addition, knockdown of Ufd1, which constitutively interacts with Npl4 to form a stable complex, also significantly increased type I interferon response to SeV infection. Together, these results suggest that Npl4-Ufd1 is the cofactor of p97 during its regulation of antiviral signaling.

To verify the above observations and further examine the regulatory effect of Npl4 in antiviral signaling, we then transfected the SeV-infected cells with increasing amounts of Npl4. As shown in Fig 2C, Npl4 potently inhibited SeV-induced activation of IFNβ- and ISRE-luciferase reporters in a dose-dependent manner. Consistent with these results, cells overexpressing Npl4 also showed substantially decreased mRNA levels of *IFNB* and *ISG56* in response to SeV infection (Fig 2D). Similar results were obtained when the cells were transfected with poly(I:C) (Appendix Fig S2E and F), indicating that Npl4 inhibits RNA/virus-induced type I interferon response. To further confirm these observations, we silenced endogenous Npl4

using a mixture of three individual siRNAs and then examined the activation of the *IFN*β and *ISRE* promoters. Knockdown of Npl4 led to a greater activation of IFNβ-, PRDIII-I-, and ISRE-luciferase reporters when compared with the control groups (Fig 2E). Accordingly, the transcription of *IFNB*, *RANTES*, and *ISG56* was promoted in Npl4-knockdown cells infected with SeV for different amounts of time (Fig 2F). Such inhibitory effects of Npl4 were also observed in cells transfected with poly(I:C) (Appendix Fig S2G and H). A subsequent rescue study showed that depletion of endogenous Npl4 by siRNA targeting its UTR sequence rendered the cells resistant to VSV infection, while back-transfection of Npl4 induced the cells to be more susceptible to VSV infection (Fig 2G). Together, these data indicate that Npl4, similar to p97, is a negative regulator of type I interferon signaling and antiviral immunity.

We next investigated whether Npl4 indeed acts as the cofactor of p97 during its negative regulation of antiviral signaling. For this purpose, we first knocked down p97 and then transfected cells with Npl4 in combination with wild-type p97 or its ATPase-defective QQ mutant. Overexpression of Npl4 alone in p97-knockdown cells failed to inhibit SeV-induced IFNβ reporter activation and *IFNB* transcription, whereas co-transfection of Npl4 with wild-type p97 but not its QQ mutant efficiently suppressed IFNβ transactivity and *IFNB* transcription (Fig 2H). Together with the above observations, these results indicate that the inhibitory role of NpI4 on type I interferon signaling is dependent on p97; that is, Npl4 *per se* acts as the cofactor of p97 during this process. Hereinafter, we mainly focused our efforts on p97 and Npl4.

Structure determination and mutational studies of the p97-Npl4 complex

To assess the atomic interactions between p97 and Npl4 in antiviral signaling, we performed structural and structure-directed mutational studies. Npl4 comprises four domains: the N-terminal UBD (amino acids 1–80) essential for interaction with p97, the central zf-Npl4 domain (amino acids 104–246) and Npl4 domain (amino acids 248–557), and the C-terminal NZF domain (amino acids 580–608) responsible for binding ubiquitin (Ye *et al*, 2003; Alam *et al*, 2004; Isaacson *et al*, 2007; Lass *et al*, 2008). In order to evaluate the functional importance of individual domains of Npl4, we generated a series of Npl4 truncation constructs: ΔNZF (amino acids 1–579), ΔUBD (amino acids 81–608), and the UBD domain alone (Figs 3A and EV1A). Compared with the wild-type Npl4, deletion of the UBD domain abolished its inhibitory effect on SeV-induced IFNβ activation and *IFNB* transcription (Fig EV1B), indicating that association of Npl4 with p97 is essential for the regulation of antiviral response.

Subsequently, the crystal structure of the drosophila Ter94 (p97) N-terminal domain in complex with the drosophila Npl4 (dNpl4) UBD was determined by the single-wavelength anomalous diffraction method to 2.0 Å resolution with a crystallographic R factor of 20.82% and a free R factor of 25.13% (Figs 3B and EV1C; Appendix Table S1). Similar to other adaptors such as p47 and FAF1, the dNpl4 UBD binds to the hydrophobic groove formed by the two N-terminal subdomains (Nn and Nc) of Ter94 (Fig 3B). The overall structures of Ter94 and dNpl4 in the complex are similar to those previously determined individually (Huyton *et al*, 2003; Dreveny *et al*, 2004; Isaacson *et al*, 2007; Hanzelmann & Schindelin, 2011; Hanzelmann *et al*, 2011). A total of 1082 $Å^2$ of the molecular surface was buried upon complex formation between dNpl4 and Ter94. The heterodimeric interface between Ter94 and dNpl4 is primarily composed of two sites termed Site 1 and Site 2 (Fig 3B). At Site 1, residues L7, R9, and R18, which are located in the β1 and β2 strands of dNpl4, form hydrophobic interactions with residue F49 from the Nn domain of Ter94. Meanwhile, hydrogen bonding and electrostatic interactions were formed between residues R9, R18, and H69 of dNpl4 and R50, D52, and Q47 of Ter94. For Site 2, residues A13 and R49 of dNpl4 were observed to interact with residues Y107 and Y140 from the Nc domain of Ter94 through hydrophobic packing, while residues A13, Q11, and R49 of dNpl4 formed hydrogen bonding and electrostatic interactions with Y107 of Ter94. In addition, R49 of dNpl4 was observed to pair with Y140 of Ter94 via a cation–π interaction. It is worth noting that all these interface residues are highly conserved between drosophila and human (Fig EV1C and D), supporting our rationale of using Ter94-dNpl4 as a substitute for p97-Npl4 in the structural analysis of this complex.

Several structures of p97 in complex with adaptors including p47, FAF1, and OTU1, were previously reported (Dreveny *et al*, 2004; Hanzelmann *et al*, 2011). Comparing these structures revealed an overall conserved fashion through which all adaptors bind to the same hydrophobic groove of p97 (Fig EV1E). However, the detailed relative positioning between p97 and its adaptors varies. It is helpful in this regard to refer to the structure of the Npl4 UBD, which was determined by nuclear magnetic resonance (NMR), and to refer to its interaction with p97, which was modeled with experimental probes (Isaacson *et al*, 2007). Compared with this NMR structure of Npl4, the crystal structure of dNpl4 determined here revealed a similar overall fold yet with significant conformational differences, especially in loops α1/β3 and β3/β4 (Fig EV1F and G). More importantly, the relative orientations between dNpl4/Npl4 and Ter94/p97 were observed to differ considerably when comparing the Ter94-dNpl4 complex structure with the previously modeled structure of p97-Npl4 (Fig EV1G). It is also noteworthy that residues Val15, Leu74, and Phe76, which were predicted to be critical for complex formation by the previous modeling, are neither evolutionarily conserved nor present in the interface of the current structure of the Ter94-dNpl4 complex. On the other hand, interface residues critical for Ter94 interaction with dNpl4 are strictly conserved across diverse species (see below). Together, these observations indicate the robust reliability of our structural analysis of the p97-Npl4 complex.

Next, we performed structure-directed mutational studies in a context of full-length human p97 and Npl4 to further evaluate the importance of individual interface residues for complex formation. Pulldown assays using purified recombinant proteins of wild-type and mutant (substitution of wild-type residue with alanine) p97 and Npl4 showed that residues of p97 engaging in either hydrophobic interactions (F52, Y110) or hydrogen bonding and electrostatic interactions (D55, Y110) are essential for Npl4 binding (Fig 3C and D). Meanwhile, mutation of the single residue R50 or multiple sites at I6, R8, R17, and R50 of Npl4 abolished its binding to p97 (Fig 3C and E). These observations were further confirmed by biolayer interferometry (Octet Red 96) using purified proteins *in vitro* (Fig EV1H and I), as well as a co-immunoprecipitation (co-IP) assay in cells (Fig 3F and G). Therefore, we chose hereinafter F52A/D55A/Y110A of p97 (termed 3A) and I6A/R8A/R17A/R50A of Npl4 (termed 4A) as representative mutants that entirely disrupt the p97-Npl4 complex.

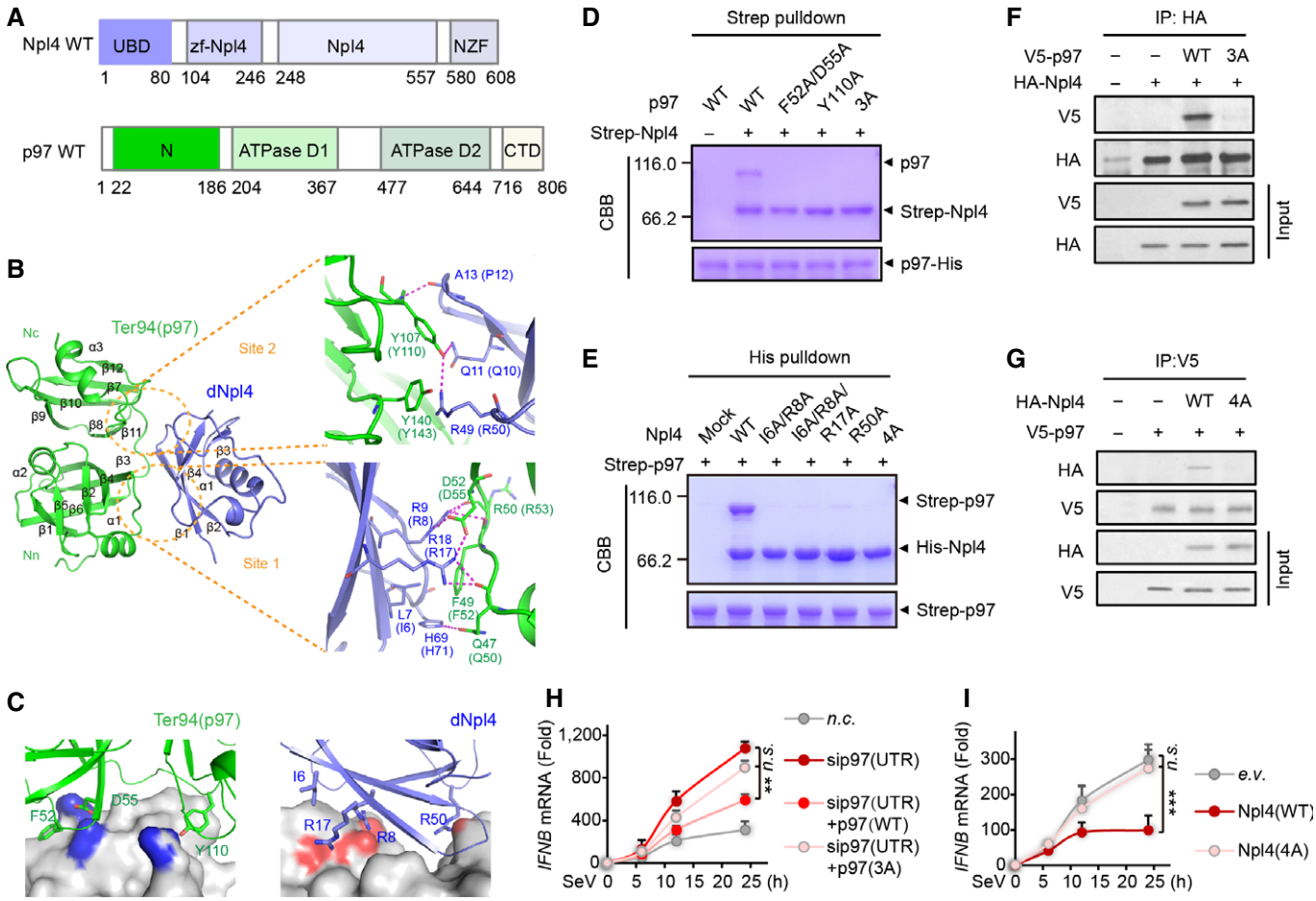

Figure 3. Structural and mutational analyses of p97-Npl4 complex in IFNβ response.

A Schematic illustration of the domain organization of human Npl4 and p97.

B Crystal structure of *Drosophila* Ter94 (homolog of human p97) in complex with *Drosophila* Npl4. Structures are colored using the same scheme as in (A) and (C). Interface residues are highlighted with ball-and-stick models. Amino acid numbering of human Npl4 and p97 is shown in the parentheses.

C Interface residues in p97 (left) and Npl4 (right) critical for complex formation.

D Strep pulldown analysis of wild-type Npl4 with various p97 mutants.

E His pulldown analysis of wild-type p97 with various Npl4 mutants.

F Co-IP analysis of wild-type Npl4 with wild-type p97 or its 3A mutant.

G Co-IP analysis of wild-type p97 with wild-type Npl4 or its 4A mutant.

H, I IFNβ transactivation (H) and *IFNB* transcription (I) in cells transfected with indicated plasmids. Error bars represent SD of data obtained in three independent experiments. Student's *t*-test was used. n.s., no significant difference; $^{**}P < 0.01$; $^{***}P < 0.001$ in comparison with control group.

Data information: 3A, p97-F52AD55AY110A; 4A, Npl4-I6AR8AR17AR50A. Other abbreviations as in Figs 1 and 2. All indicated proteins used in pulldown assays were purified recombinant proteins (same below).
See also Fig EV1.
Source data are available online for this figure.

Finally, we transfected HEK293T cells with wild-type or mutant p97 and Npl4. Upon SeV infection, overexpression of wild-type p97 but not its 3A mutant in cells depleted of endogenous p97 inhibited IFNβ transactivation and *IFNB* transcription (Fig 3H). Meanwhile, transfection of wild-type Npl4 but not its 4A mutant suppressed IFNβ promoter activation and *IFNB* transcription in cells after SeV infection for different durations of time (Fig 3I). Taken together, these results further validate our structural analysis and indicate that direct interaction between p97 and Npl4 to form a complex is essential for their suppressive role in antiviral signaling.

The p97-Npl4 complex promotes degradation of RIG-I

Given that p97 is an AAA ATPase relevant to the control of protein stability, we surmised that p97-Npl4 might function by targeting components of RLR-mediated antiviral signaling such as the RIG-I pathway for proteasome degradation. To test this possibility, we first determined the protein levels of RIG-I, MAVS, and IRF3 in cells transfected with short hairpin RNA (shRNA) interfering the transcription of p97 (Fig 4A). Knockdown of p97 markedly increased poly(I:C)-induced RIG-I expression when compared with scramble.

The protein level of MAVS was also increased, while the total level of IRF3 protein remained unchanged. Consistent with the increased level of RIG-I and MAVS, the phosphorylation of IRF3 was obviously enhanced (Fig 4A). In addition, overexpression of Npl4 significantly reduced poly(I:C)-induced expression of RIG-I and MAVS when compared with the control, leading to decreased phosphorylation of IRF3 (Fig 4B). Moreover, depletion of Npl4 significantly increased the poly(I:C)-induced expression of the proteins RIG-I and MAVS with enhanced IRF3 phosphorylation, as was found for the effect of knocking down p97, but did not affect the protein levels of TBK1, IKKε, and IRF3, suggesting that p97-Npl4 specifically targets the proteins RIG-I and MAVS (Fig 4C). Meanwhile, a similar effect was observed for depletion of Ufd1, while knockdown of p47, another p97 cofactor, did not cause such an effect, again indicating that Npl4-Ufd1, and specifically NpI4-Ufd1, is required for p97 regulation of RIG-I antiviral signaling (Fig EV2A and B).

Next, we examined whether regulation of RIG-I antiviral signaling by p97-Npl4 is dependent on proteasomal degradation. A real-time PCR assay showed that overexpression of Npl4 in cells transfected with poly(I:C) did not affect the mRNA levels of RIG-I (Fig EV2C). Furthermore, RIG-I protein level reduction mediated by p97 together with NpI4 was largely blocked when cells were treated with MG132, a proteasome inhibitor (Fig 4D and E), suggesting that p97-Npl4 regulates the RIG-I protein level through proteasome degradation. Subsequently, we analyzed the potential regulatory role of p97-Npl4 on K48-linked polyubiquitination of RIG-I.

The p97-Npl4 complex is required for K48 ubiquitination of RIG-I

As mentioned before, a mechanism commonly proposed to explain how p97 functions is that, with the help of various cofactors, p97 is recruited to the ubiquitinated substrates and targets them for proteasome degradation. Thus, depletion of p97 and its cofactors would lead to an accumulation of ubiquitinated substrates (Ballar *et al*, 2006; Alexandru *et al*, 2008; Meerang *et al*, 2011; Raman *et al*, 2011; Kim *et al*, 2013; Chan *et al*, 2014; Li *et al*, 2014). To examine the potential effect of p97-Npl4 on K48-linked polyubiquitination of RIG-I, we transfected Flag-tagged RIG-I into HEK293T cells with wild-type p97/Npl4 or their mutants that disrupt complex formation. Unexpectedly, co-transfection of Flag-RIG-I with wild-type p97, but not of its 3A mutant defective in binding Npl4, in p97-depleted cells led to accumulation of K48-linked RIG-I polyubiquitination in these cells (Figs 4F and EV2D). Similarly, overexpression of wild-type Npl4 enhanced K48-linked polyubiquitination of RIG-I compared to overexpression of its 4A mutant, which is unable to bind p97 (Figs 4G and EV2E). Consistent with these results, knockdown of either p97 or Npl4 substantially decreased K48-linked ubiquitination of RIG-I (Fig 4H and I). Taken together, these results indicate that p97-Npl4 suppresses antiviral response by promoting K48-linked polyubiquitination and proteasomal degradation of RIG-I, and this process depends on the direct interaction between p97 and Npl4.

RNF125 is the E3 ligase required for p97-Npl4-mediated RIG-I turnover

To explore the underlying mechanism of p97-Npl4-related degradation of RIG-I, we set out to identify the potential E3 ligase responsible for RIG-I turnover during this process. So far, two E3 ligases, RNF125 and c-Cbl, have been identified to mediate K48-linked ubiquitination of RIG-I (Arimoto *et al*, 2007; Chen *et al*, 2013). To assess these two ligases, we first designed two groups of shRNAs targeting RNF125 and c-Cbl respectively. The knockdown efficiency of each of these shRNAs was validated by real-time PCR analysis (Fig EV3A). According to the results of a dual-luciferase reporter assay, depletion of endogenous RNF125 abrogated the ability of Npl4 to downregulate IFNβ promoter activity induced by SeV infection, whereas knockdown of c-Cbl had no such effect (Fig 5A), suggesting that the inhibition of RIG-I antiviral signaling by Npl4 is dependent on RNF125. Similarly, Npl4 failed to suppress IFNβ transactivation triggered by overexpression of RIG-I CARDs in cells depleted of RNF125, but not c-Cbl (Fig 5B). Consistent with these observations, overexpression of Npl4 significantly decreased poly(I:C)-induced accumulation of RIG-I protein, while depletion of endogenous RNF125 impaired such an effect of Npl4 (Fig 5C). Together, these findings suggest that RNF125 is specifically required for p97-Npl4-mediated inhibition of RIG-I antiviral signaling.

We next examined the ubiquitination levels of RIG-I in cells transfected with Npl4 and/or RNF125. Consistent with the aforementioned results, overexpression of Npl4 significantly increased K48-linked ubiquitination of RIG-I, while co-expression of Npl4 with RNF125 further enhanced this effect (Fig 5D), indicating that Npl4 acts synergistically with RNF125 to facilitate K48-linked ubiquitination of RIG-I. Consistently, Npl4 could no longer increase K48-linked ubiquitination of RIG-I when endogenous RNF125 was depleted (Fig EV3B). These observations were further confirmed by a QPCR assay showing that co-transfection of Npl4 and RNF125 suppressed IFNβ transcription to a larger extent than did Npl4 or RNF125 alone (Fig 5E). Taken together, these results indicate that p97-Npl4 inhibits RIG-I-related type I interferon response by promoting RNF125-mediated K48-linked ubiquitination of RIG-I.

Figure 4. p97-Npl4 inhibits RIG-I signaling by promoting its proteasomal degradation.

A Immunoblot analysis of RIG-I and MAVS, as well as phosphorylated (p-) or total IRF3 in p97-depleted cells after treatment with poly(I:C) for different durations.
B Immunoblot analysis of the indicated proteins in cells overexpressing Npl4 after treatment with poly(I:C) for different durations.
C Immunoblot analysis of RIG-I, MAVS, p-TBK1, TBK1, IKKε, and p-IRF3 and IRF3 in shNpl4 cells after transfection with poly(I:C) for different durations.
D Protein levels of RIG-I in sip97 cells overexpressing p97 after being treated with MG132.
E Protein levels of RIG-I in cells overexpressing Npl4 after being treated with MG132.
F Ubiquitination of RIG-I in sip97 cells transfected with wild-type p97 and its 3A mutant.
G Ubiquitination of RIG-I in cells transfected with wild-type Npl4 and its 4A mutant.
H, I Ubiquitination of RIG-I in sip97 (H) and siNpl4 (I) cells after being challenged with SeV.

Data information: For abbreviations, see Figs 1–3.
See also Fig EV2.
Source data are available online for this figure.

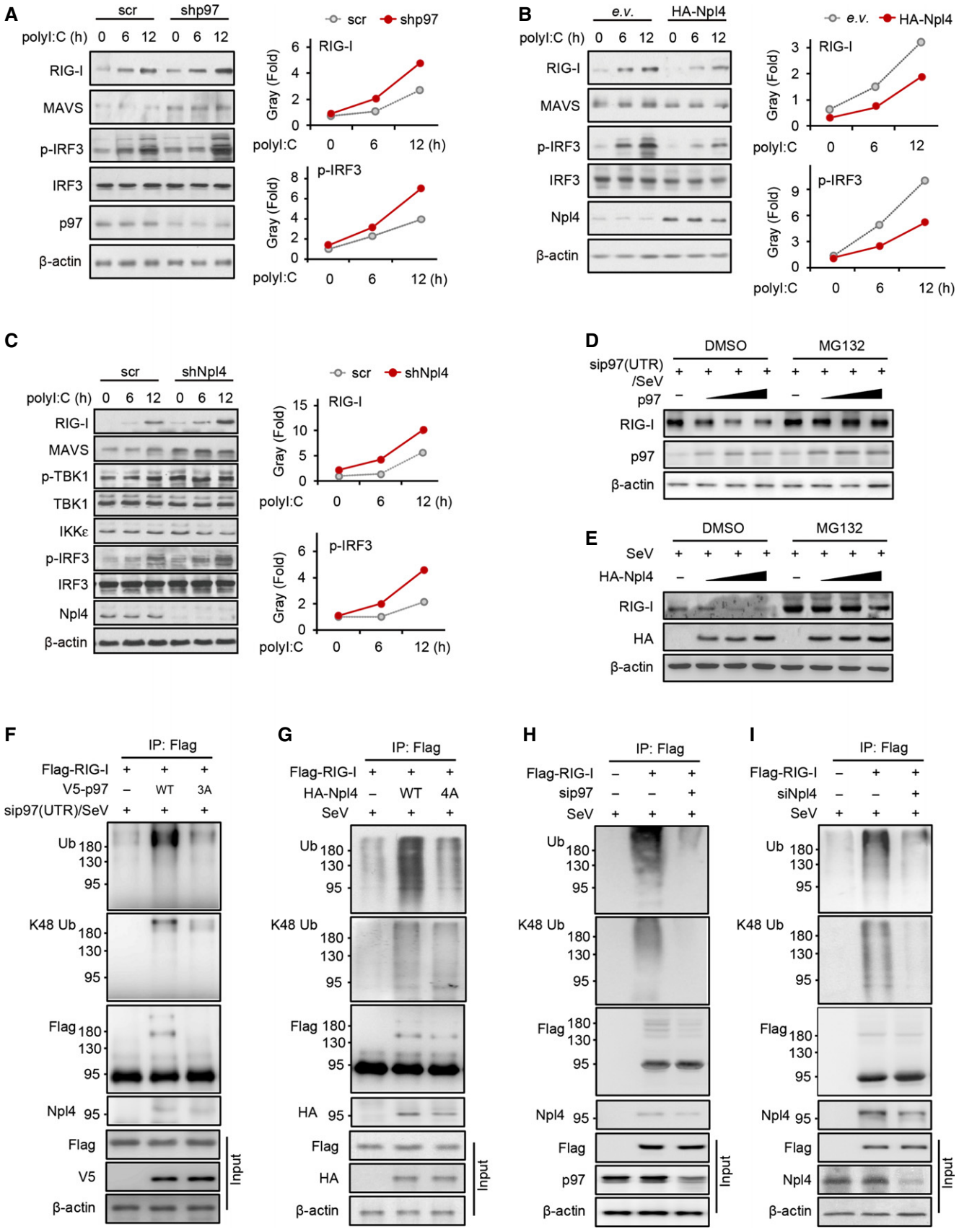

Figure 4.

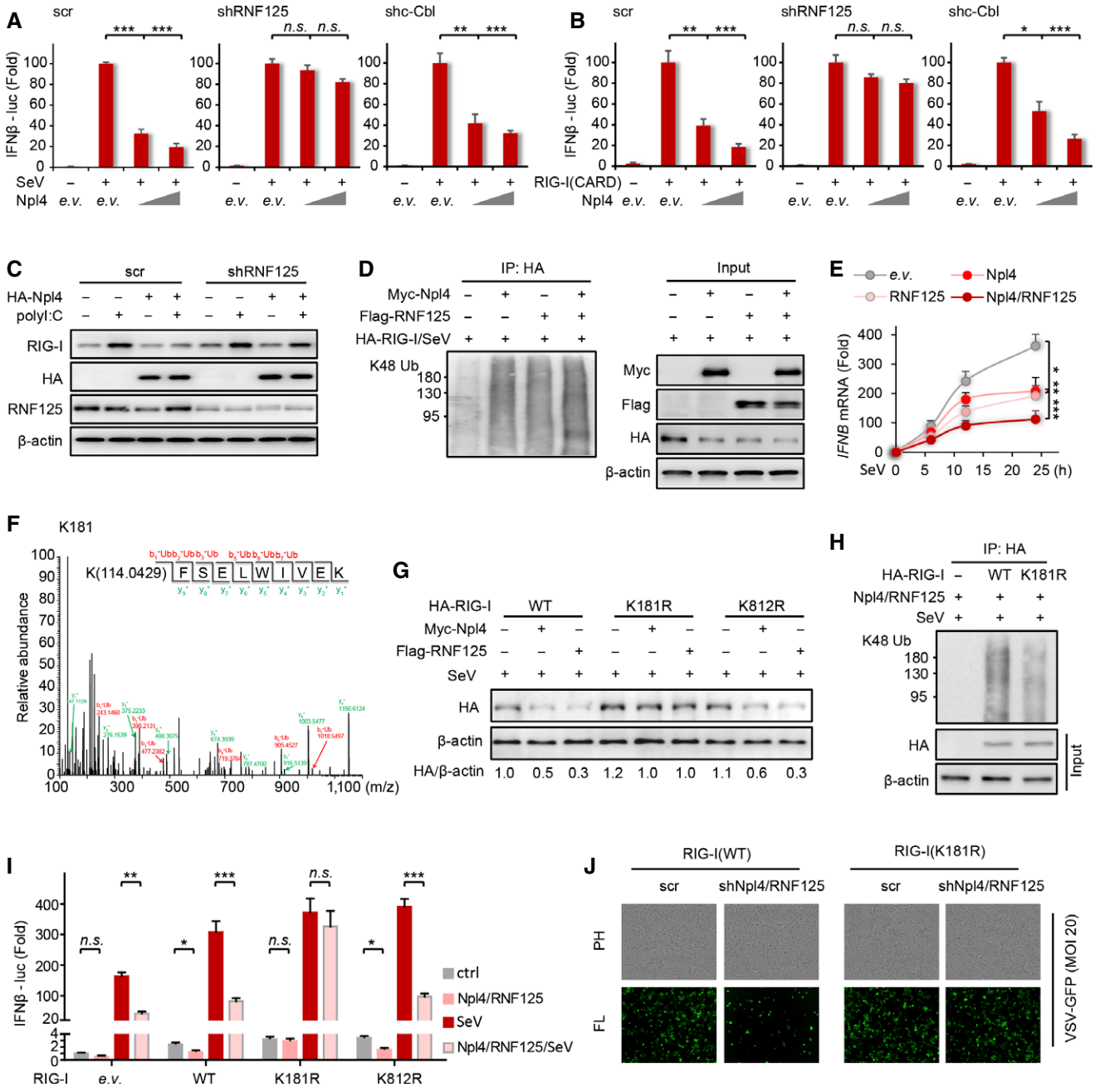

Figure 5. RNF125 is essential for p97-Npl4 inhibition of RIG-I signaling.

A Luciferase activity detected in HEK293T cells transfected with an IFNβ luciferase reporter, plus scramble, shRNF125, or shc-Cbl, and increasing doses of Npl4 after SeV infection.

B Luciferase analysis of IFNβ promoter activity in cells transfected with the tandem CARDs of RIG-I, plus scramble, shRNF125, or shc-Cbl, and increasing doses of Npl4.

C Protein levels of RIG-I in shRNF125 cells with or without transfection of Npl4.

D Ubiquitination of RIG-I in cells transfected with Npl4 in combination with RNF125 after being challenged with SeV.

E mRNA levels of *IFNB* in SeV-infected cells after transfection with Npl4 or RNF125 or both.

F Mass spectrometric analysis of ubiquitination sites of RIG-I after co-transfection with RNF125 and HA-K48Ub.

G Immunoblotting analysis of RIG-I in cells transfected with wild-type or mutant RIG-I and Npl4 or RNF125.

H Ubiquitination of wild-type or mutant RIG-I in cells transfected with Npl4 and RNF125.

I IFNβ transactivity in SeV-infected cells transfected with wild-type or mutant RIG-I in combination with Npl4 and RNF125.

J Fluorescence microscopy (GFP) of VSV-GFP-infected cells after transfection with shNpl4 and shRNF125, as well as wild-type RIG-I and its mutants.

Data information: Error bars represent SD of data obtained in three independent experiments. One-way analysis of variance (ANOVA) and Student's *t*-test were used. n.s., no significant difference; $*P < 0.05$; $**P < 0.01$; $***P < 0.001$ in comparison with control group. For abbreviations, see Figs 1 and 2.
See also Fig EV3.
Source data are available online for this figure.

K181 is the key site for RNF125-p97-Npl4-mediated ubiquitination of RIG-I

While a previous study identified RNF125 as an E3 ligase that contributes to K48-linked ubiquitination of RIG-I (Arimoto *et al*, 2007), its specific target site remains unknown. To determine the RNF125-mediated ubiquitination site(s) on RIG-I, we carried out a mass spectrometry analysis with and without overexpression of RNF125. Previously, c-Cbl was reported to catalyze K48-linked ubiquitination of RIG-I on lysine 812 (Chen *et al*, 2013). We thus used K812 of RIG-I as a control in our study. MS analysis revealed K181, but not K812, as a candidate site for K48-linked ubiquitination of RIG-I catalyzed by RNF125 (Fig 5F). To verify this result, wild-type and mutant RIG-I were each co-transfected with Npl4 or RNF125 in SeV-infected cells. An immunoblotting assay showed that overexpression of Npl4 or RNF125 in SeV-infected cells significantly downregulated the protein levels of wild-type RIG-I as well as of its K812R mutant, but not that of the RIG-I K181R mutant (Fig 5G), indicating that K181 of RIG-I is a major site targeted by RNF125 and p97-Npl4 for regulation of RIG-I-related antiviral signaling. Moreover, Npl4 could not enhance K48-linked ubiquitination of the RIG-I K181R mutant as it does on wild-type RIG-I (Figs 5H and EV3C). Consistent with these observations, inclusion of RNF125 and Npl4 together significantly inhibited IFNβ promoter activation induced by wild-type RIG-I or its K812R mutant, but failed to inhibit that induced by the K181R mutant of RIG-I (Fig 5I).

Next, the antiviral effects of wild-type RIG-I and its K181R mutant were each monitored upon depletion of Npl4 and RNF125. When compared with scramble, knockdown of Npl4 and RNF125 further inhibited VSV infection (MOI, 20) in cells transfected with wild-type RIG-I, but failed to do so in cells transfected with the K181R mutant of RIG-I, again indicating that K181 *per se* is the targeted site (Fig 5J). We then examined the local structural environment of K181 in RIG-I and found this site to be in the vicinity of K172, a major site for K63-linked ubiquitination critical for RIG-I activation; it was also observed to be near T170, a phosphorylation site implicated in negative regulation of RIG-I signaling (Fig EV3D). Taken together, these results strongly indicate that K181 of RIG-I is the key site for RNF125/p97-Npl4-mediated RIG-I ubiquitination, and suggest that K48-linked ubiquitination at K181 could be regulated by posttranslational modifications of K172 and K170 (see more below).

The p97-Npl4 complex directly interacts with both RIG-I and RNF125

To further dissect the mechanism by which p97-Npl4 mediates inhibition of RIG-I antiviral signaling, we sought to determine whether the p97-Npl4 complex physically associates with RIG-I and with RNF125. A co-IP assay in HEK293T cells showed that endogenous RIG-I interacted with endogenous Npl4, and such interaction was substantially increased upon being infected with SeV (Fig 6A). Meanwhile, the previously reported association of RIG-I with RNF125 (Arimoto *et al*, 2007) was also detected. Consistent with the above results, confocal microscopy showed enhanced colocalization of endogenous Npl4 and RIG-I upon SeV infection (Fig 6B). Furthermore, an *in vitro* pulldown assay using purified recombinant proteins of Npl4 and RIG-I indicates that the interaction between Npl4 and RIG-I is a direct one (Fig 6C).

Next, we mapped the specific domains of RIG-I and Npl4 mediating their association. Three truncated forms of RIG-I were generated and co-expressed with full-length Npl4 in HEK293T cells. A co-IP assay showed that the portion of RIG-I containing the CARDs (amino acids 1-238) interacts with Npl4 as indicated by the band next to the red asterisk in Fig 6D, whereas the helicase and carboxyl-terminal domains of RIG-I were not involved in this interaction (Fig 6D). In addition, two deletion mutants of Npl4 were constructed and co-expressed with full-length RIG-I. The resulting co-IP assay showed that deletion of the NZF domain completely disrupted the interaction of Npl4 with RIG-I, whereas deletion of the UBD did not affect this interaction (Figs 6E and EV1A), suggesting that the NZF domain is essential for association between Npl4 and RIG-I. These observations were further confirmed by an *in vitro* pulldown assay showing a direct interaction between Npl4 and the CARDs of RIG-I (Fig EV4A).

Finally, we sought to determine whether RNF125 interacts with p97. An endogenous IP assay showed that RNF125 could not only associate with RIG-I, but also interact with p97 (Fig 6F). Subsequently, we used purified recombinant proteins to further assess the interactions among p97-Npl4, RIG-I, and RNF125. p97 was readily pulled down by RNF125 but not by an MBP control, indicating a direct interaction between p97 and RNF125 (Fig 6G). Furthermore, RNF125 could directly pull down RIG-I; and the p97-Npl4 complex further promoted the interaction between RNF125 and RIG-I (Fig 6H). Together, these observations suggest that the p97-Npl4 complex physically associates with both RIG-I and RNF125 and that Npl4 directly interacts with the CARDs even without ubiquitination of RIG-I.

RIG-I interaction with Npl4 is enhanced by exposure and K63 ubiquitination of the CARDs

Since Npl4 could directly bind to non-ubiquitinated RIG-I CARDs, while SeV greatly enhanced the binding of NpI4 to RIG-I in cells, we then investigated how such an interaction is regulated upon viral infection. Given that binding of dsRNA triggers a conformational change of RIG-I that results in its oligomerization and the exposure of the CARDs, we first evaluated whether dsRNA could enhance Npl4 interaction with non-ubiquitinated RIG-I. To this end, we performed an *in vitro* pulldown assay using purified recombinant proteins of Npl4 and RIG-I and synthesized dsRNA that binds to RIG-I and induces its dimerization (Feng *et al*, 2013). The interaction between Npl4 and RIG-I was obviously increased when dsRNA and ATP were added (Fig 6I). This result suggests that a viral infection-triggered conformational change of RIG-I could facilitate its interaction with Npl4 by exposing the CARDs.

Considering the key role of K63-linked polyubiquitin in RIG-I antiviral signaling, we next studied the potential function of K63-linked ubiquitination in regulating the interaction of Npl4 with RIG-I CARDs. It is well established that the E3 ubiquitin ligase TRIM25 activates RIG-I by generation of K63-linked polyubiquitin chains covalently attached to K172 of RIG-I (Gack *et al*, 2007). Meanwhile, separated K63-linked polyubiquitin chains can bind to RIG-I noncovalently for synergistic activation (Zeng *et al*, 2010). Furthermore, T170 was found constitutively phosphorylated under physiological conditions, preventing RIG-I from binding to TRIM25 and MAVS (Gack *et al*, 2010). Moreover, phosphorylation of T170 not only

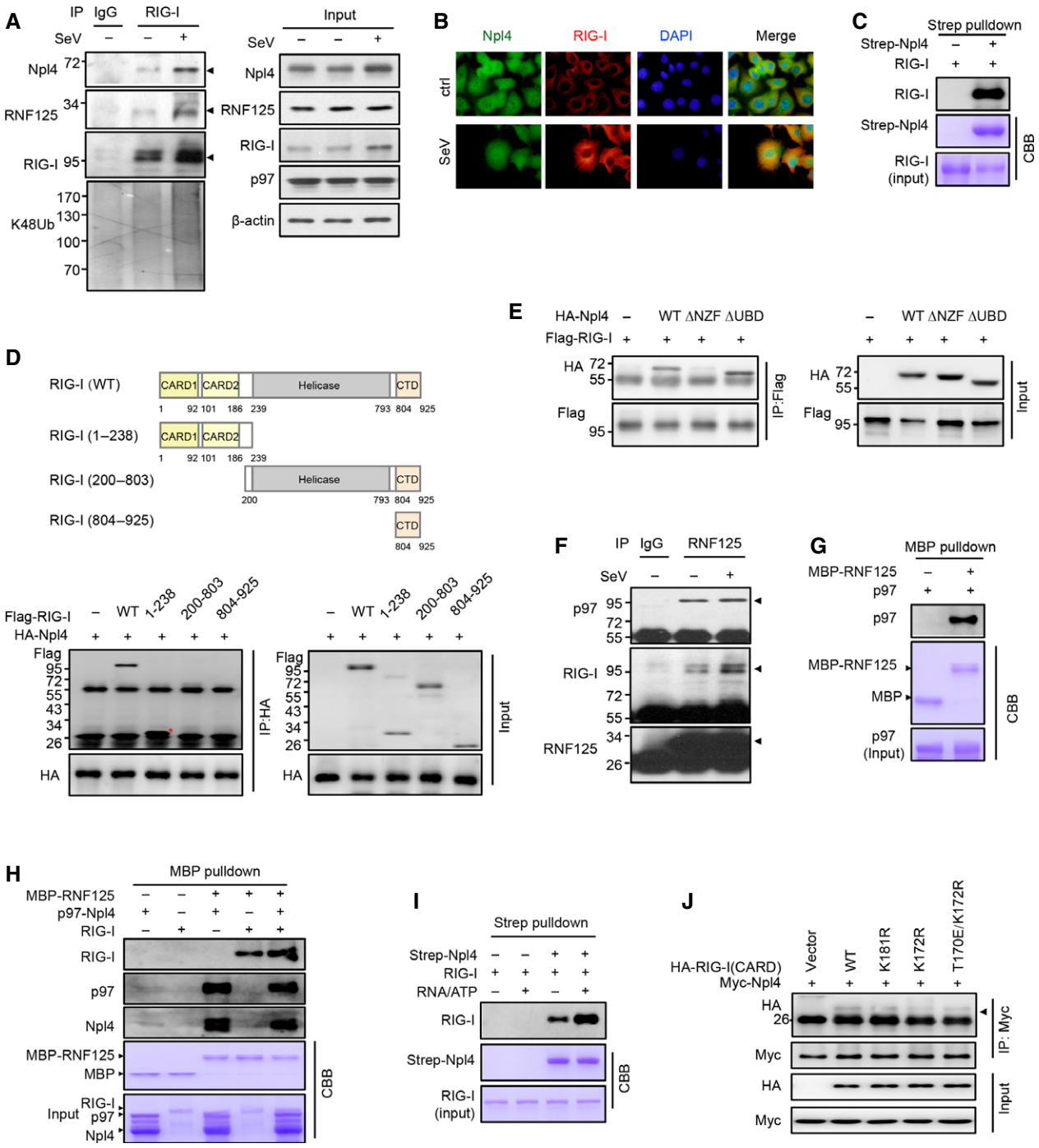

Figure 6. p97-Npl4 directly interacts with both RIG-I and RNF125.

A Endogenous co-IP assays for Npl4 and RIG-I with or without SeV infection.

B Colocalization of Npl4 and RIG-I with or without SeV infection.

C *In vitro* pulldown assay to assess the direct interaction between Npl4 and RIG-I.

D, E Domain mapping of Npl4 and RIG-I interaction by co-IP experiment. Red asterisk in panel D marks the position of RIG-I (1-238).

F Endogenous co-IP assay for p97 and RNF125 with or without SeV infection.

G *In vitro* pulldown assay to assess the direct interaction between p97 and RNF125.

H *In vitro* pulldown assay to assess the interaction between RIG-I and RNF125 with or without the p97-Npl4 complex.

I Pulldown assay to assess the effect of dsRNA/ATP on direct interaction between RIG-I and Npl4.

J Co-IP assay for Npl4 with RIG-I-CARDs and its mutants.

See also Fig EV4.

Source data are available online for this figure.

impaired ubiquitination of RIG-I at K172, but also abolished the non-covalent binding between RIG-I and K63-linked polyubiquitin chains. Based on these studies, we constructed two RIG-I-CARDs mutants (K172R and T170E/K172R) to evaluate the possible effect of K63-linked ubiquitination on the interaction between RIG-I and Npl4.

We then transfected cells with wild-type or mutant RIG-I-CARDs, together with Npl4. When compared with wild-type RIG-I-CARDs, the K172R mutant that blocks K63-linked ubiquitination of RIG-I showed significantly decreased binding to Npl4 (Fig 6J). Similarly, the double mutation T170E/K172R that blocks both covalent ubiquitination of RIG-I and non-covalent binding of K63-linked polyubiquitin chains to RIG-I impaired the interaction between RIG-I and Npl4. These results indicate that K63-linked ubiquitination of RIG-I facilitates the binding of Npl4 to RIG-I. Next, we co-transfected cells with wild-type or mutant RIG-I-CARDs, Npl4, TRIM25, and ubiquitin. Consistent with previous report, TRIM25 promoted ubiquitination of wild-type RIG-I-CARDs, but not the K172R and T170E/K172R mutants (Fig EV4B). More importantly, the altered ubiquitination levels of RIG-I-CARDs appear to be correlated with Npl4 binding to RIG-I. These observations were further confirmed by an *in vitro* pulldown assay showing that Npl4 binds stronger to the wild-type RIG-I-CARDs when compared with the T170E/K172R mutant RIG-I-CARDs (Fig EV4C). Taken together, these results indicate that K63-linked ubiquitination of RIG-I may greatly enhance its interaction with the p97 complex.

Targeting p97-Npl4 promotes RIG-I antiviral signaling and protects mice from VSV infection

To further corroborate our mechanistic study of the regulation of the RIG-I antiviral signaling by p97-Npl4 and to explore the therapeutic potential of this complex, we took advantage of the recently developed p97 inhibitors DBeQ and NMS-873 (Fig 7A), which bind distinct sites of p97 to specifically turn off its ATPase activity (Chou & Deshaies, 2011; Chou *et al*, 2011; Magnaghi *et al*, 2013). As expected, both DBeQ and NMS-873 increased, in a dose-dependent manner, IFNβ promoter transactivation in cells infected with SeV (Fig 7B), confirming that the ATPase activity of p97 is essential for its regulatory function in RIG-I antiviral signaling. Consistent with these results, DBeQ and NMS-873 inhibited K48-linked ubiquitination of endogenous RIG-I upon virus challenge (Fig 7C), again indicating that p97 promotes ubiquitination of RIG-I in an ATPase-dependent manner. Moreover, cells treated with either DBeQ or NMS-873 were endowed with enhanced resistance to VSV infection (Fig 7D). Together, these results further support the notion that p97-Npl4 inhibits RIG-I antiviral signaling by promoting K48-linked ubiquitination and proteasomal degradation of RIG-I and that p97-Npl4 could be targeted for therapeutic purposes.

We next assessed the potential therapeutic effects of p97 inhibitors by treating mice intravenously. Strikingly, the average survival rates of VSV-infected mice treated with DBeQ and with NMS-873 were each significantly enhanced in a dose-dependent manner when compared with that of mice treated with saline (Fig 7E). Consistent with this observation, VSV titers in serum of mice treated with DBeQ and in serum of mice treated with NMS-873 were much lower than those of control mice (Fig 7F). Consistently, IFNβ production was significantly increased in VSV-infected mice that were treated with DBeQ or NMS-873 compared with that of control mice (Fig EV5A). Moreover, DBeQ and NMS-873 did not exhibit a detectable toxicity (no significant weight change of mice treated with these compounds) at the indicated dosage that displayed clear evidence of an antiviral effect (Fig EV5B). Together, these observations clearly indicate that therapeutic targeting of the p97-Npl4 complex can enhance antiviral response and protect mice from viral infection.

Discussion

As a sensor of RNA viruses, RIG-I needs to have its activation accurately regulated. Upon infection, the conformation of RIG-I is converted from an auto-suppressed state to an active configuration, enclosing viral RNA within a central cavity formed by the helicase and C-terminal domains; this conformational change also exposes the N-terminal CARDs to solvent and thus allows them to bind MAVS and affect downstream signaling (Kolakofsky *et al*, 2012). Sustained RIG-I-MAVS signaling is then attenuated by different types of negative regulators after clearance of invasive virus. For example, the deubiquitinases CYLD (Friedman *et al*, 2008; Zhang *et al*, 2008) and USP21 (Fan *et al*, 2014) can reverse K63-linked ubiquitination of RIG-I and thus inhibit its downstream signaling. Meanwhile, RIG-I is also regulated at the level of protein degradation as shown by studies on RNF125 and c-Cbl (Arimoto *et al*, 2007; Chen *et al*, 2013).

The ATP-driven chaperone p97 has been found to participate in a wide range of independent cellular processes (Hauler *et al*, 2012; Yamanaka *et al*, 2012). Previously, p97 was implicated in the regulation of both classical and alternative NF-κB signaling pathways (Dai *et al*, 1998; Asai *et al*, 2002), indicating the functional relevance of p97 in inflammatory responses. In this work, we have identified the p97-Npl4-Ufd1 complex as a novel negative regulator of RIG-I-mediated antiviral signaling and uncovered a non-canonical role for p97 in the control of protein stability. Mechanistically, the p97 complex directly interacts with both RIG-I and the E3 ligase RNF125 to promote K48-linked ubiquitination of RIG-I at K181 and therefore facilitate its proteasomal degradation. During this process, the NZF domain of Npl4 and the CARDs of RIG-I are critical for the interaction between Npl4 and RIG-I, but this interaction does not depend on the UBD of Npl4, which is instead essential for association with p97. Meanwhile, RNF125 was shown to interact with both RIG-I and p97. Compared with the well-studied canonical function of p97—that is, "remodeling and transporting ubiquitinated proteins"—our results suggest that the p97 complex may also act as an adaptor to bridge substrate proteins with E3 ligase and thus facilitate the ubiquitination process.

A structure-directed mutational study, as well as analyses using p97 inhibitors, revealed that an intact state of the p97 complex, with its ATPase activity being functional, is required for the regulation of RIG-I antiviral signaling. Moreover, lysine 181 of RIG-I was identified as a primary site for RNF125-p97-mediated downregulation of RIG-I antiviral signaling. In this regard, it is worth noting that K181 (site for K48-linked ubiquitination) is adjacent to other critical regulatory sites in the 3D structure, namely K172 (site for K63-linked ubiquitination) and T170 (site for phosphorylation) in the RIG-I CARDs. Such a conformation may allow for cross talk among different types of PTM to regulate RIG-I signaling, which could involve not only E3 ubiquitin ligase, but also deubiquitinase, or even kinase and phosphatase.

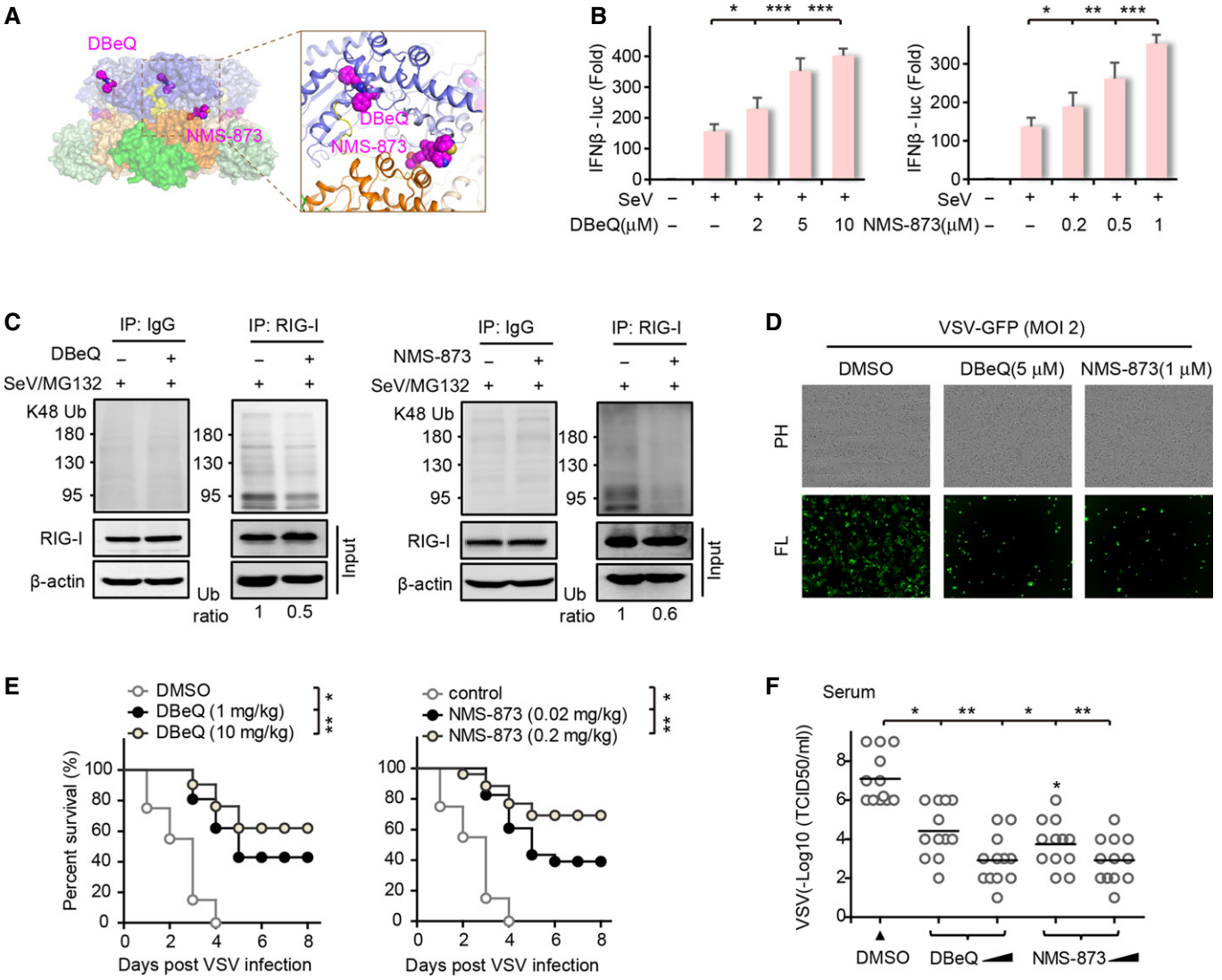

Figure 7. Enzymatic inhibition of p97 protects mice from viral infection.

A Hypothetical structural model of p97 hexamer bound with its inhibitors DBeQ and NMS-873.

B IFNβ transactivation in SeV-infected cells after treatment with DBeQ or NMS-873.

C Ubiquitination of RIG-I in HEK293T cells after treatment with DBeQ or NMS-873.

D Viral loads in drug-treated cells infected with VSV-GFP.

E Survival of VSV-infected mice after treatment with different doses of DBeQ or NMS-873 (n = 20). The mice were intranasally challenged with VSV. Two days after infection, tissue fluids were collected from the mice. Equal volumes (10 ml) of serum were added to HEK293 cell culture media and incubated for 24 h, followed by the viral titer being calculated.

F Viral titer in the serum of VSV-infected mice treated with DBeQ or NMS-873. Horizontal lines represent the means.

Data information: Error bars represent SD of data obtained in three independent experiments. Log-rank test and Student's t-test were used for survival curves and continuous variables, respectively. n.s., no significant difference; *P < 0.05; **P < 0.01; ***P < 0.001 in comparison with control group.
See also Fig EV5.

Based on our results, we propose a working model in which the p97 complex helps to recruit RNF125 and facilitate K48-linked ubiquitination and proteasomal degradation of RIG-I, thus dampening the antiviral response (Fig EV5C). The p97 complex is able to bind non-ubiquitinated RIG-I, yet viral infection-induced activation of RIG-I could markedly strengthen such binding through conformational exposure and K63-linked ubiquitination of the CARDs. It is likely that the p97 complex may help to avoid spontaneous RIG-I signaling or maintain a proper threshold at basal level. Upon viral infection, RIG-I undergoes a conformational change that exposes its CARDs. Subsequent K63-linked polyubiquitination of RIG-I rapidly enhances its binding with the p97 complex, which in turn recruits RNF125 for K48-linked polyubiquitination of RIG-I and subsequent degradation to "turn off" the signaling. As such, a prolonged RIG-I signaling would be terminated right after an effective antiviral response is elicited.

It has been well established that the ATPase p97 possesses segregase activity able to segregate its substrates from their binding partners or cellular surfaces (Meyer *et al*, 2012). In this regard, we also observed a negative regulatory role of p97-Npl4 on the stability of the protein MAVS. Such a phenomenon is not surprising considering that RNF125 has also been implicated in regulating the turnover of MAVS (Arimoto *et al*, 2007). Furthermore, we found that RIG-I binding to the p97 cofactor Npl4 could be significantly enhanced by dsRNA-triggered oligomerization (therefore exposing the CARDs) and K63-linked ubiquitination of RIG-I, two key events for subsequent interaction with and activation of MAVS. Thus, it is reasonable to speculate that the p97 complex may also regulate the disassembly of RIG-I-MAVS signaling complex.

Notably, p97 has been emerging as a potential target for cancer therapy on account of its levels being positively correlated with prognosis of multiple types of cancer including gastric carcinoma (Yamamoto *et al*, 2003a), non-small cell lung carcinoma (Yamamoto *et al*, 2004a; Valle *et al*, 2011), hepatocellular carcinoma (Yamamoto *et al*, 2003b; Liu *et al*, 2012), follicular thyroid cancer (Yamamoto *et al*, 2005), prostate cancer (Tsujimoto *et al*, 2004), and pancreatic endocrine neoplasm (Yamamoto *et al*, 2004b). Inhibitors of p97 have been experimentally indicated to induce cancer cell death, making them potent adjuvants for preventing tumor growth and metastasis. For instance, DBeQ, a reversible ATP-competitive p97 inhibitor, can selectively induce apoptosis in human cancer cells (Chou & Deshaies, 2011; Chou *et al*, 2011). NMS-859, a covalent inhibitor of p97 that blocks its ATP-binding site, can impede the proliferation of cancer cells (Magnaghi *et al*, 2013). Recently, NMS-873 was reported as the most potent and specific p97 inhibitor to date, whose binding to p97 was shown to hamper its allosteric conformational changes (Magnaghi *et al*, 2013). NMS-873 showed cell-killing activity in hematological tumors as well as a wide variety of solid tumors with IC_{50} values ranging from 0.08 to 2 μM.

Our studies showed that targeting the p97 complex either through depletion of p97 or its cofactor Npl4-Ufd1 or by treatment with p97 inhibitors enhanced RIG-I-mediated antiviral immune responses, highlighting the p97-Npl4-Ufd1 complex as a novel target for antiviral therapy. In particular, the results in VSV-infected mice treated with p97 inhibitors validate their protective effect against viral infection. We did not observe significant weight change for mice treated with DBeQ or NMS-873 in our study, although further work is needed to systematically assess the potential toxic effects of such inhibitors as drugs. Considering that most p97 inhibitors were initially developed to treat cancer and that antiviral treatment is a routine procedure for cancer patients after surgery, it would be beneficial to use a p97 inhibitor as both an anticancer and antiviral agent. Further efforts aimed at developing novel inhibitors targeting the p97-Npl4-Ufd1 complex, which could result in more specific drugs than are currently available, are certainly warranted.

Materials and Methods

Cells, reagents, and antibodies

Human HEK293, HEK293T, and HeLa cells were purchased from the Cell Resource Center (Institute of Life Sciences, Chinese Academy of Sciences). Cells were maintained in Dulbecco's minimum essential medium (DMEM), supplemented with 10% fetal calf serum (FBS) and penicillin/streptomycin. Sendai virus (SeV) was kindly provided by Dr. Hong-Bing Shu (Wuhan University). NMS-873 was purchased from Selleck Chemicals (Houston, TX). Poly(I:C), DBeQ, and antibodies specific for Flag, Myc, and β-actin were purchased from Sigma (St. Louis, MO). Antibodies specific for p97, RIG-I, MAVS, p-TBK, TBK, IKKε, p-IRF3, IRF3, and K48Ub were purchased from Cell Signaling (Danvers, MA); those for HA, ubiquitin, and RNF125 were from Santa Cruz (Santa Cruz, CA) and those for Npl4 (IF) were from Novus Biologicals (Littleton, CO). An antibody specific for Npl4 (IP and WB) was bought from Abcam (Cambridge, UK).

Plasmids and protein purification

Mammalian expression vectors for HA-/myc-Npl4, V5-p97, and HA-/Flag-Rig-I were described previously (Feng *et al*, 2013; Zhang *et al*, 2013). The drosophila Ter94 N domain (amino acids 20-186) and the dNpl4 UBD (amino acids 1-77) were cloned into the vector HT-pET28a, which contains a 6× His tag and a TEV protease cleavage site at the N-terminus. Proteins were expressed in *E. coli* BL21 (DE3) Codon Plus cells (Stratagene) by induction with 0.5 mM isopropyl β-D-thiogalactopyranoside at OD_{600} = 1.0 in Terrific Broth medium for 18 h at 16°C. The cells were harvested and lysed by using a high-pressure homogenizer (JNBIO3000 plus) at 1300 bar in lysis buffer containing 20 mM Hepes pH 7.5, 500 mM NaCl, 5% glycerol, 20 mM imidazole, 1 mM DTT, and 1 mM PMSF. Proteins were then purified by nickel affinity chromatography and finally eluted by the lysis buffer plus 500 mM imidazole. After TEV cleavage to remove the His tag, the protein was applied to a HiLoad 16/60 Superdex 200 column (GE Healthcare) pre-equilibrated with a buffer containing 20 mM Hepes pH 7.5, 100 mM NaCl, and 1 mM DTT. Purified Ter94 N and dNpl4 UBD, in an equimolar ratio, were mixed and applied to the gel filtration column once more to obtain the binary complex.

Selenomethionine (SeMet)-labeled Ter94 N and dNpl4 UBD were expressed in *E. coli* BL21 (DE3) Codon Plus cells, which were cultured in M9 medium containing an amino acid supplement (lysine, phenylalanine, and threonine to a final concentration of 100 mg/l, isoleucine, leucine, and valine to a final concentration of 50 mg/l, and L-SeMet to a final concentration of 60 mg/l). SeMet-labeled protein was purified in the same way as the native protein described above.

Human full-length p97 (amino acids 1–806), Npl4 (amino acids 1–608), and RIG-I (amino acids 1–925) were separately cloned into the vector pET28a, leading to the target protein with a C-terminal His tag. Human full-length p97 (amino acids 1–806) and Npl4 (amino acids 1–608) were also cloned into the vector pET51b, which contains a Strep tag at the N-terminus. All the proteins were expressed and purified according to the methods described above.

Structure determination and refinement

The Ter94 N–Npl4 UBD complex was concentrated to 25 mg/ml for the crystallization screen. Crystals were obtained by sitting-drop vapor diffusion at 16°C using a reservoir solution consisting of 0.1 M Tris pH 8.5, 23% w/v polyethylene glycol 3350, and 0.2 M

ammonium sulfate. Crystals were cryoprotected by soaking them in a solution composed of 0.1 M Tris pH 8.5, 23% w/v polyethylene glycol 3350, 0.2 M ammonium sulfate, and 10% glycerol and then flash-frozen in liquid nitrogen.

Diffraction data were collected on beamlines BL17U at Shanghai Synchrotron Radiation Facility (SSRF) and 1W2B at Beijing Synchrotron Radiation Facility (BSRF) and processed using HKL2000. The structure was solved by the single-wavelength anomalous diffraction method from a SeMet derivative with the program AutoSol in Phenix (Adams *et al*, 2010). The structure was refined using phenix.refine, and model building was performed in Coot (McCoy *et al*, 2007; Emsley *et al*, 2010). The coordinate files and structure factors for the p97-Npl4 complex crystal structure were deposited in the Protein Data Bank under accession code 4RV0.

Viral infection of mice

For infection, 7- to 8-week-old mice were narcotized and then intranasally inoculated with VSV. Negative controls included saline and PBS. Clinical symptoms were observed 2–8 days post-inoculation, and the analyses described below were performed. All procedures for animal experimentation were performed in accordance with the Institutional Animal Care and Use Committee guidelines of the Animal Core Facility of the Institutes of Biochemistry and Cell Biology (SIBCB). The approval ID for using the animals was No. 081 by the Animal Core Facility of SIBCB.

Viral titer assay

After VSV infection, peripheral blood and tissue were collected to obtain serum and tissue fluid, respectively. For the VSV titer assay, sera or tissue fluids were added into culture media of HEK293 cells, and the viral titer was determined by a standard plaque assay.

Confocal imaging

HeLa cells were plated on coverslips in 6-well plates and transfected with the indicated plasmids. Twenty-four hours later, the cells were treated with or without SeV (MOI = 1) for 24 h. Coverslips with the cells were washed once with PBS and fixed in 3.7% formaldehyde in PBS for 15 min. After permeabilization with Triton X-100 (0.25%) in PBS for 15 min, the cells were blocked with PBS containing BSA (5%) for 1 h and then incubated with primary antibodies for 1 h. After three separate washes, the cells were incubated with secondary antibody for another hour and then stained with DAPI for 2 min. The coverslips were washed extensively and fixed on slides. Images of these cells were captured using a Leica laser scanning confocal microscope (Leica TCS SP2 AOBS).

Statistical analysis

Statistical analysis was performed using the SAS statistical software package (9.1.3). Data are presented as mean ± SD. One-way analysis of variance (ANOVA) and Student's *t*-test were used for continuous variables. Survival curves were calculated according to the Kaplan–Meier method; survival analysis was performed using the log-rank test. $P < 0.05$ was considered significantly different.

Expanded View for this article is available online:
http://emboj.embopress.org

Acknowledgements
We thank the staff at beamlines BL17U of Shanghai Synchrotron Radiation Facility and 1W2B of Beijing Synchrotron Radiation Facility for help with data collection. We thank Drs. Jin-Qiu Zhou, Hongbing Shu, Zhengfan Jiang, Bing Sun, and Chen Wang for their generous support. This work was supported by the 973 Program of the Ministry of Science and Technology of China (2012CB910204), the National Natural Science Foundation of China (31270808, 31300734, 31470736, 31470868, 91442125, 91542125), the Science and Technology Commission of Shanghai Municipality (11JC14140000, 13ZR1446400), and the "Cross and Cooperation in Science and Technology Innovation Team" Project of the Chinese Academy of Sciences, the Youth Innovation Promotion Association of Chinese Academy of Sciences, and the Knowledge Innovation Program of Shanghai Institutes for Biological Sciences, Chinese Academy of Sciences (2014KIP202).

Author contributions
QH performed biochemical and structural studies. SJ, ZheZ, and YW performed cellular experiments and *in vivo* analyses. ZS performed structural analysis. CL and XM performed mass spectrometry analysis. XS, WW, RZ, and YZ contributed to experimental design. CCLW contributed to data analysis. QH, XS, SJ, and ZhaZ wrote the manuscript. ZhaZ supervised the project.

Conflict of interest
The authors have filed patents for therapeutic targeting of p97 and Npl4 (201510362643.5, 201510359075.3, 201510359088.0).

References

Adams PD, Afonine PV, Bunkoczi G, Chen VB, Davis IW, Echols N, Headd JJ, Hung LW, Kapral GJ, Grosse-Kunstleve RW, McCoy AJ, Moriarty NW, Oeffner R, Read RJ, Richardson DC, Richardson JS, Terwilliger TC, Zwart PH (2010) PHENIX: a comprehensive Python-based system for macromolecular structure solution. *Acta Crystallogr D Biol Crystallogr* 66: 213 – 221

Alam SL, Sun J, Payne M, Welch BD, Blake BK, Davis DR, Meyer HH, Emr SD, Sundquist WI (2004) Ubiquitin interactions of NZF zinc fingers. *EMBO J* 23: 1411 – 1421

Alexandru G, Graumann J, Smith GT, Kolawa NJ, Fang R, Deshaies RJ (2008) UBXD7 binds multiple ubiquitin ligases and implicates p97 in HIF1alpha turnover. *Cell* 134: 804 – 816

Arimoto K, Takahashi H, Hishiki T, Konishi H, Fujita T, Shimotohno K (2007) Negative regulation of the RIG-I signaling by the ubiquitin ligase RNF125. *Proc Natl Acad Sci USA* 104: 7500 – 7505

Asai T, Tomita Y, Nakatsuka S, Hoshida Y, Myoui A, Yoshikawa H, Aozasa K (2002) VCP (p97) regulates NFkappaB signaling pathway, which is important for metastasis of osteosarcoma cell line. *Jpn J Cancer Res* 93: 296 – 304

Ballar P, Shen Y, Yang H, Fang S (2006) The role of a novel p97/valosin-containing protein-interacting motif of gp78 in endoplasmic reticulum-associated degradation. *J Biol Chem* 281: 35359 – 35368

Barbalat R, Ewald SE, Mouchess ML, Barton GM (2011) Nucleic acid recognition by the innate immune system. *Annu Rev Immunol* 29: 185 – 214

Cao K, Nakajima R, Meyer HH, Zheng Y (2003) The AAA-ATPase Cdc48/p97 regulates spindle disassembly at the end of mitosis. *Cell* 115: 355 – 367

Chan NC, den Besten W, Sweredoski MJ, Hess S, Deshaies RJ, Chan DC (2014) Degradation of the deubiquitinating enzyme USP33 is mediated by p97 and the ubiquitin ligase HERC2. *J Biol Chem* 289: 19789 – 19798

Chen W, Han C, Xie B, Hu X, Yu Q, Shi L, Wang Q, Li D, Wang J, Zheng P, Liu Y, Cao X (2013) Induction of Siglec-G by RNA viruses inhibits the innate immune response by promoting RIG-I degradation. *Cell* 152: 467 – 478

Chou TF, Brown SJ, Minond D, Nordin BE, Li K, Jones AC, Chase P, Porubsky PR, Stoltz BM, Schoenen FJ, Patricelli MP, Hodder P, Rosen H, Deshaies RJ (2011) Reversible inhibitor of p97, DBeQ, impairs both ubiquitin-dependent and autophagic protein clearance pathways. *Proc Natl Acad Sci USA* 108: 4834 – 4839

Chou TF, Deshaies RJ (2011) Development of p97 AAA ATPase inhibitors. *Autophagy* 7: 1091 – 1092

Dai RM, Chen E, Longo DL, Gorbea CM, Li CC (1998) Involvement of valosin-containing protein, an ATPase Co-purified with IkappaBalpha and 26 S proteasome, in ubiquitin-proteasome-mediated degradation of IkappaBalpha. *J Biol Chem* 273: 3562 – 3573

Dreveny I, Kondo H, Uchiyama K, Shaw A, Zhang X, Freemont PS (2004) Structural basis of the interaction between the AAA ATPase p97/VCP and its adaptor protein p47. *EMBO J* 23: 1030 – 1039

Emsley P, Lohkamp B, Scott WG, Cowtan K (2010) Features and development of Coot. *Acta Crystallogr D Biol Crystallogr* 66: 486 – 501

Fan Y, Mao R, Yu Y, Liu S, Shi Z, Cheng J, Zhang H, An L, Zhao Y, Xu X, Chen Z, Kogiso M, Zhang D, Zhang P, Jung JU, Li X, Xu G, Yang J (2014) USP21 negatively regulates antiviral response by acting as a RIG-I deubiquitinase. *J Exp Med* 211: 313 – 328

Feng M, Ding Z, Xu L, Kong L, Wang W, Jiao S, Shi Z, Greene MI, Cong Y, Zhou Z (2013) Structural and biochemical studies of RIG-I antiviral signaling. *Protein Cell* 4: 142 – 154

Friedman CS, O'Donnell MA, Legarda-Addison D, Ng A, Cardenas WB, Yount JS, Moran TM, Basler CF, Komuro A, Horvath CM, Xavier R, Ting AT (2008) The tumour suppressor CYLD is a negative regulator of RIG-I-mediated antiviral response. *EMBO Rep* 9: 930 – 936

Fu X, Ng C, Feng D, Liang C (2003) Cdc48p is required for the cell cycle commitment point at Start via degradation of the G1-CDK inhibitor Far1p. *J Cell Biol* 163: 21 – 26

Gack MU, Shin YC, Joo CH, Urano T, Liang C, Sun L, Takeuchi O, Akira S, Chen Z, Inoue S, Jung JU (2007) TRIM25 RING-finger E3 ubiquitin ligase is essential for RIG-I-mediated antiviral activity. *Nature* 446: 916 – 920

Gack MU, Nistal-Villan E, Inn KS, Garcia-Sastre A, Jung JU (2010) Phosphorylation-mediated negative regulation of RIG-I antiviral activity. *J Virol* 84: 3220 – 3229

Gao D, Yang YK, Wang RP, Zhou X, Diao FC, Li MD, Zhai ZH, Jiang ZF, Chen DY (2009) REUL is a novel E3 ubiquitin ligase and stimulator of retinoic-acid-inducible gene-I. *PLoS ONE* 4: e5760

Hanzelmann P, Buchberger A, Schindelin H (2011) Hierarchical binding of cofactors to the AAA ATPase p97. *Structure* 19: 833 – 843

Hanzelmann P, Schindelin H (2011) The structural and functional basis of the p97/valosin-containing protein (VCP)-interacting motif (VIM): mutually exclusive binding of cofactors to the N-terminal domain of p97. *J Biol Chem* 286: 38679 – 38690

Hauler F, Mallery DL, McEwan WA, Bidgood SR, James LC (2012) AAA ATPase p97/VCP is essential for TRIM21-mediated virus neutralization. *Proc Natl Acad Sci USA* 109: 19733 – 19738

Heo JM, Livnat-Levanon N, Taylor EB, Jones KT, Dephoure N, Ring J, Xie J, Brodsky JL, Madeo F, Gygi SP, Ashrafi K, Glickman MH, Rutter J (2010) A stress-responsive system for mitochondrial protein degradation. *Mol Cell* 40: 465 – 480

Hetzer M, Meyer HH, Walther TC, Bilbao-Cortes D, Warren G, Mattaj IW (2001) Distinct AAA-ATPase p97 complexes function in discrete steps of nuclear assembly. *Nat Cell Biol* 3: 1086 – 1091

Higashiyama H, Hirose F, Yamaguchi M, Inoue YH, Fujikake N, Matsukage A, Kakizuka A (2002) Identification of ter94, Drosophila VCP, as a modulator of polyglutamine-induced neurodegeneration. *Cell Death Differ* 9: 264 – 273

Huyton T, Pye VE, Briggs LC, Flynn TC, Beuron F, Kondo H, Ma J, Zhang X, Freemont PS (2003) The crystal structure of murine p97/VCP at 3.6A. *J Struct Biol* 144: 337 – 348

Indig FE, Partridge JJ, von Kobbe C, Aladjem MI, Latterich M, Bohr VA (2004) Werner syndrome protein directly binds to the AAA ATPase p97/VCP in an ATP-dependent fashion. *J Struct Biol* 146: 251 – 259

Isaacson RL, Pye VE, Simpson P, Meyer HH, Zhang X, Freemont PS, Matthews S (2007) Detailed structural insights into the p97-Npl4-Ufd1 interface. *J Biol Chem* 282: 21361 – 21369

Jarosch E, Taxis C, Volkwein C, Bordallo J, Finley D, Wolf DH, Sommer T (2002) Protein dislocation from the ER requires polyubiquitination and the AAA-ATPase Cdc48. *Nat Cell Biol* 4: 134 – 139

Jiang F, Ramanathan A, Miller MT, Tang GQ, Gale M Jr, Patel SS, Marcotrigiano J (2011) Structural basis of RNA recognition and activation by innate immune receptor RIG-I. *Nature* 479: 423 – 427

Ju JS, Fuentealba RA, Miller SE, Jackson E, Piwnica-Worms D, Baloh RH, Weihl CC (2009) Valosin-containing protein (VCP) is required for autophagy and is disrupted in VCP disease. *J Cell Biol* 187: 875 – 888

Kato H, Takahasi K, Fujita T (2011) RIG-I-like receptors: cytoplasmic sensors for non-self RNA. *Immunol Rev* 243: 91 – 98

Kawai T, Takahashi K, Sato S, Coban C, Kumar H, Kato H, Ishii KJ, Takeuchi O, Akira S (2005) IPS-1, an adaptor triggering RIG-I- and Mda5-mediated type I interferon induction. *Nat Immunol* 6: 981 – 988

Kawai T, Akira S (2008) Toll-like receptor and RIG-I-like receptor signaling. *Ann N Y Acad Sci* 1143: 1 – 20

Kawai T, Akira S (2010) The role of pattern-recognition receptors in innate immunity: update on Toll-like receptors. *Nat Immunol* 11: 373 – 384

Kim NC, Tresse E, Kolaitis RM, Molliex A, Thomas RE, Alami NH, Wang B, Joshi A, Smith RB, Ritson GP, Winborn BJ, Moore J, Lee JY, Yao TP, Pallanck L, Kundu M, Taylor JP (2013) VCP is essential for mitochondrial quality control by PINK1/Parkin and this function is impaired by VCP mutations. *Neuron* 78: 65 – 80

Kobayashi T, Manno A, Kakizuka A (2007) Involvement of valosin-containing protein (VCP)/p97 in the formation and clearance of abnormal protein aggregates. *Genes Cells* 12: 889 – 901

Kolakofsky D, Kowalinski E, Cusack S (2012) A structure-based model of RIG-I activation. *RNA* 18: 2118 – 2127

Kondo H, Rabouille C, Newman R, Levine TP, Pappin D, Freemont P, Warren G (1997) p47 is a cofactor for p97-mediated membrane fusion. *Nature* 388: 75 – 78

Konno H, Yamamoto T, Yamazaki K, Gohda J, Akiyama T, Semba K, Goto H, Kato A, Yujiri T, Imai T, Kawaguchi Y, Su B, Takeuchi O, Akira S, Tsunetsugu-Yokota Y, Inoue J (2009) TRAF6 establishes innate immune responses by activating NF-kappaB and IRF7 upon sensing cytosolic viral RNA and DNA. *PLoS ONE* 4: e5674

Kowalinski E, Lunardi T, McCarthy AA, Louber J, Brunel J, Grigorov B, Gerlier D, Cusack S (2011) Structural basis for the activation of innate immune pattern-recognition receptor RIG-I by viral RNA. *Cell* 147: 423 – 435

Krick R, Bremer S, Welter E, Schlotterhose P, Muehe Y, Eskelinen EL, Thumm M (2010) Cdc48/p97 and Shp1/p47 regulate autophagosome biogenesis in concert with ubiquitin-like Atg8. *J Cell Biol* 190: 965 – 973

Lass A, McConnell E, Fleck K, Palamarchuk A, Wojcik C (2008) Analysis of Npl4 deletion mutants in mammalian cells unravels new Ufd1-interacting motifs and suggests a regulatory role of Npl4 in ERAD. *Exp Cell Res* 314: 2715 – 2723

Latterich M, Frohlich KU, Schekman R (1995) Membrane fusion and the cell cycle: Cdc48p participates in the fusion of ER membranes. *Cell* 82: 885 – 893

Li JM, Wu H, Zhang W, Blackburn MR, Jin J (2014) The p97-UFD1L-NPL4 protein complex mediates cytokine-induced IkappaBalpha proteolysis. *Mol Cell Biol* 34: 335 – 347

Liu S, Chen ZJ (2011) Expanding role of ubiquitination in NF-kappaB signaling. *Cell Res* 21: 6 – 21

Liu Y, Hei Y, Shu Q, Dong J, Gao Y, Fu H, Zheng X, Yang G (2012) VCP/p97, down-regulated by microRNA-129-5p, could regulate the progression of hepatocellular carcinoma. *PLoS ONE* 7: e35800

Luo D, Ding SC, Vela A, Kohlway A, Lindenbach BD, Pyle AM (2011) Structural insights into RNA recognition by RIG-I. *Cell* 147: 409 – 422

Maelfait J, Beyaert R (2012) Emerging role of ubiquitination in antiviral RIG-I signaling. *Microbiol Mol Biol Rev* 76: 33 – 45

Magnaghi P, D'Alessio R, Valsasina B, Avanzi N, Rizzi S, Asa D, Gasparri F, Cozzi L, Cucchi U, Orrenius C, Polucci P, Ballinari D, Perrera C, Leone A, Cervi G, Casale E, Xiao Y, Wong C, Anderson DJ, Galvani A *et al* (2013) Covalent and allosteric inhibitors of the ATPase VCP/p97 induce cancer cell death. *Nat Chem Biol* 9: 548 – 556

McCoy AJ, Grosse-Kunstleve RW, Adams PD, Winn MD, Storoni LC, Read RJ (2007) Phaser crystallographic software. *J Appl Crystallogr* 40: 658 – 674

Meerang M, Ritz D, Paliwal S, Garajova Z, Bosshard M, Mailand N, Janscak P, Hubscher U, Meyer H, Ramadan K (2011) The ubiquitin-selective segregase VCP/p97 orchestrates the response to DNA double-strand breaks. *Nat Cell Biol* 13: 1376 – 1382

Meyer H, Bug M, Bremer S (2012) Emerging functions of the VCP/p97 AAA-ATPase in the ubiquitin system. *Nat Cell Biol* 14: 117 – 123

Meylan E, Curran J, Hofmann K, Moradpour D, Binder M, Bartenschlager R, Tschopp J (2005) Cardif is an adaptor protein in the RIG-I antiviral pathway and is targeted by hepatitis C virus. *Nature* 437: 1167 – 1172

Mouysset J, Deichsel A, Moser S, Hoege C, Hyman AA, Gartner A, Hoppe T (2008) Cell cycle progression requires the CDC-48UFD-1/NPL-4 complex for efficient DNA replication. *Proc Natl Acad Sci USA* 105: 12879 – 12884

Nakhaei P, Genin P, Civas A, Hiscott J (2009) RIG-I-like receptors: sensing and responding to RNA virus infection. *Semin Immunol* 21: 215 – 222

Nishikori S, Yamanaka K, Sakurai T, Esaki M, Ogura T (2008) p97 Homologs from *Caenorhabditis elegans*, CDC-48.1 and CDC-48.2, suppress the aggregate formation of huntingtin exon1 containing expanded polyQ repeat. *Genes Cells* 13: 827 – 838

Oganesyan G, Saha SK, Guo B, He JQ, Shahangian A, Zarnegar B, Perry A, Cheng G (2006) Critical role of TRAF3 in the Toll-like receptor-dependent and -independent antiviral response. *Nature* 439: 208 – 211

O'Neill LA, Bowie AG (2010) Sensing and signaling in antiviral innate immunity. *Curr Biol* 20: R328 – R333

Onoguchi K, Yoneyama M, Fujita T (2011) Retinoic acid-inducible gene-I-like receptors. *J Interferon Cytokine Res* 31: 27 – 31

Oshiumi H, Matsumoto M, Hatakeyama S, Seya T (2009) Riplet/RNF135, a RING finger protein, ubiquitinates RIG-I to promote interferon-beta induction during the early phase of viral infection. *J Biol Chem* 284: 807 – 817

Oshiumi H, Matsumoto M, Seya T (2012) Ubiquitin-mediated modulation of the cytoplasmic viral RNA sensor RIG-I. *J Biochem* 151: 5 – 11

Partridge JJ, Lopreiato JO Jr, Latterich M, Indig FE (2003) DNA damage modulates nucleolar interaction of the Werner protein with the AAA ATPase p97/VCP. *Mol Biol Cell* 14: 4221 – 4229

Paz S, Vilasco M, Werden SJ, Arguello M, Joseph-Pillai D, Zhao T, Nguyen TL, Sun Q, Meurs EF, Lin R, Hiscott J (2011) A functional C-terminal TRAF3-binding site in MAVS participates in positive and negative regulation of the IFN antiviral response. *Cell Res* 21: 895 – 910

Rabinovich E, Kerem A, Frohlich KU, Diamant N, Bar-Nun S (2002) AAA-ATPase p97/Cdc48p, a cytosolic chaperone required for endoplasmic reticulum-associated protein degradation. *Mol Cell Biol* 22: 626 – 634

Ramadan K, Bruderer R, Spiga FM, Popp O, Baur T, Gotta M, Meyer HH (2007) Cdc48/p97 promotes reformation of the nucleus by extracting the kinase Aurora B from chromatin. *Nature* 450: 1258 – 1262

Raman M, Havens CG, Walter JC, Harper JW (2011) A genome-wide screen identifies p97 as an essential regulator of DNA damage-dependent CDT1 destruction. *Mol Cell* 44: 72 – 84

Saha SK, Pietras EM, He JQ, Kang JR, Liu SY, Oganesyan G, Shahangian A, Zarnegar B, Shiba TL, Wang Y, Cheng G (2006) Regulation of antiviral responses by a direct and specific interaction between TRAF3 and Cardif. *EMBO J* 25: 3257 – 3263

Sasagawa Y, Otani M, Higashitani N, Higashitani A, Sato K, Ogura T, Yamanaka K (2009) Caenorhabditis elegans p97 controls germline-specific sex determination by controlling the TRA-1 level in a CUL-2-dependent manner. *J Cell Sci* 122: 3663 – 3672

Satoh T, Kato H, Kumagai Y, Yoneyama M, Sato S, Matsushita K, Tsujimura T, Fujita T, Akira S, Takeuchi O (2010) LGP2 is a positive regulator of RIG-I- and MDA5-mediated antiviral responses. *Proc Natl Acad Sci USA* 107: 1512 – 1517

Seth RB, Sun L, Ea CK, Chen ZJ (2005) Identification and characterization of MAVS, a mitochondrial antiviral signaling protein that activates NF-kappaB and IRF 3. *Cell* 122: 669 – 682

Song EJ, Yim SH, Kim E, Kim NS, Lee KJ (2005) Human Fas-associated factor 1, interacting with ubiquitinated proteins and valosin-containing protein, is involved in the ubiquitin-proteasome pathway. *Mol Cell Biol* 25: 2511 – 2524

Song C, Wang Q, Li CC (2007) Characterization of the aggregation-prevention activity of p97/valosin-containing protein. *Biochemistry* 46: 14889 – 14898

Takeuchi O, Akira S (2010) Pattern recognition receptors and inflammation. *Cell* 140: 805 – 820

Tanaka A, Cleland MM, Xu S, Narendra DP, Suen DF, Karbowski M, Youle RJ (2010) Proteasome and p97 mediate mitophagy and degradation of mitofusins induced by Parkin. *J Cell Biol* 191: 1367 – 1380

Tresse E, Salomons FA, Vesa J, Bott LC, Kimonis V, Yao TP, Dantuma NP, Taylor JP (2010) VCP/p97 is essential for maturation of ubiquitin-containing autophagosomes and this function is impaired by mutations that cause IBMPFD. *Autophagy* 6: 217 – 227

Tsujimoto Y, Tomita Y, Hoshida Y, Kono T, Oka T, Yamamoto S, Nonomura N, Okuyama A, Aozasa K (2004) Elevated expression of valosin-containing protein (p97) is associated with poor prognosis of prostate cancer. *Clin Cancer Res* 10: 3007 – 3012

Valle CW, Min T, Bodas M, Mazur S, Begum S, Tang D, Vij N (2011) Critical role of VCP/p97 in the pathogenesis and progression of non-small cell lung carcinoma. *PLoS ONE* 6: e29073

Vesa J, Su H, Watts GD, Krause S, Walter MC, Martin B, Smith C, Wallace DC, Kimonis VE (2009) Valosin containing protein associated inclusion body myopathy: abnormal vacuolization, autophagy and cell fusion in myoblasts. *Neuromuscul Disord* 19: 766 – 772

Wang Q, Shinkre BA, Lee JG, Weniger MA, Liu Y, Chen W, Wiestner A, Trenkle WC, Ye Y (2010) The ERAD inhibitor Eeyarestatin I is a bifunctional compound with a membrane-binding domain and a p97/VCP inhibitory group. *PLoS ONE* 5: e15479

Wang Y, Tong X, Ye X (2012) Ndfip1 negatively regulates RIG-I-dependent immune signaling by enhancing E3 ligase Smurf1-mediated MAVS degradation. *J Immunol* 189: 5304 – 5313

Xu LG, Wang YY, Han KJ, Li LY, Zhai Z, Shu HB (2005) VISA is an adapter protein required for virus-triggered IFN-beta signaling. *Mol Cell* 19: 727 – 740

Xu S, Peng G, Wang Y, Fang S, Karbowski M (2011) The AAA-ATPase p97 is essential for outer mitochondrial membrane protein turnover. *Mol Biol Cell* 22: 291 – 300

Yamamoto S, Tomita Y, Hoshida Y, Takiguchi S, Fujiwara Y, Yasuda T, Yano M, Nakamori S, Sakon M, Monden M, Aozasa K (2003a) Expression level of valosin-containing protein is strongly associated with progression and prognosis of gastric carcinoma. *J Clin Oncol* 21: 2537 – 2544

Yamamoto S, Tomita Y, Nakamori S, Hoshida Y, Nagano H, Dono K, Umeshita K, Sakon M, Monden M, Aozasa K (2003b) Elevated expression of valosin-containing protein (p97) in hepatocellular carcinoma is correlated with increased incidence of tumor recurrence. *J Clin Oncol* 21: 447 – 452

Yamamoto S, Tomita Y, Hoshida Y, Iizuka N, Monden M, Yamamoto S, Iuchi K, Aozasa K (2004a) Expression level of valosin-containing protein (p97) is correlated with progression and prognosis of non-small-cell lung carcinoma. *Ann Surg Oncol* 11: 697 – 704

Yamamoto S, Tomita Y, Nakamori S, Hoshida Y, Iizuka N, Okami J, Nagano H, Dono K, Umeshita K, Sakon M, Ishikawa O, Ohigashi H, Aozasa K, Monden M (2004b) Valosin-containing protein (p97) and Ki-67 expression is a useful marker in detecting malignant behavior of pancreatic endocrine neoplasms. *Oncology* 66: 468 – 475

Yamamoto S, Tomita Y, Uruno T, Hoshida Y, Qiu Y, Iizuka N, Nakamichi I, Miyauchi A, Aozasa K (2005) Increased expression of valosin-containing protein (p97) is correlated with disease recurrence in follicular thyroid cancer. *Ann Surg Oncol* 12: 925 – 934

Yamanaka K, Okubo Y, Suzaki T, Ogura T (2004) Analysis of the two p97/VCP/Cdc48p proteins of *Caenorhabditis elegans* and their suppression of polyglutamine-induced protein aggregation. *J Struct Biol* 146: 242 – 250

Yamanaka K, Sasagawa Y, Ogura T (2012) Recent advances in p97/VCP/Cdc48 cellular functions. *Biochim Biophys Acta* 1823: 130 – 137

Ye Y, Meyer HH, Rapoport TA (2001) The AAA ATPase Cdc48/p97 and its partners transport proteins from the ER into the cytosol. *Nature* 414: 652 – 656

Ye Y, Meyer HH, Rapoport TA (2003) Function of the p97-Ufd1-Npl4 complex in retrotranslocation from the ER to the cytosol: dual recognition of nonubiquitinated polypeptide segments and polyubiquitin chains. *J Cell Biol* 162: 71 – 84

Yoshida R, Takaesu G, Yoshida H, Okamoto F, Yoshioka T, Choi Y, Akira S, Kawai T, Yoshimura A, Kobayashi T (2008) TRAF6 and MEKK1 play a pivotal role in the RIG-I-like helicase antiviral pathway. *J Biol Chem* 283: 36211 – 36220

You F, Sun H, Zhou X, Sun W, Liang S, Zhai Z, Jiang Z (2009) PCBP2 mediates degradation of the adaptor MAVS via the HECT ubiquitin ligase AIP4. *Nat Immunol* 10: 1300 – 1308

Zeng W, Sun L, Jiang X, Chen X, Hou F, Adhikari A, Xu M, Chen ZJ (2010) Reconstitution of the RIG-I pathway reveals a signaling role of unanchored polyubiquitin chains in innate immunity. *Cell* 141: 315 – 330

Zhang M, Wu X, Lee AJ, Jin W, Chang M, Wright A, Imaizumi T, Sun SC (2008) Regulation of IkappaB kinase-related kinases and antiviral responses by tumor suppressor CYLD. *J Biol Chem* 283: 18621 – 18626

Zhang Z, Lv X, Yin WC, Zhang X, Feng J, Wu W, Hui CC, Zhang L, Zhao Y (2013) Ter94 ATPase complex targets k11-linked ubiquitinated ci to proteasomes for partial degradation. *Dev Cell* 25: 636 – 644

